

CRWMS/M&O

Design Analysis Cover Sheet

Complete only applicable items.

①

QA: L

Page: 1 Of: 61

2. DESIGN ANALYSIS TITLE			
Initial Waste Package Probabilistic Criticality Analysis: Uncanistered Fuel (TBV-059-WPD) (SCP8:NA)			
3. DOCUMENT IDENTIFIER (Including Rev. No.)		4. REV. NO.	5. TOTAL PAGES
B00000000-01717-2200-00079 REV00		00	61
6. TOTAL ATTACHMENTS	7. ATTACHMENT NUMBERS - NO. OF PAGES IN EACH		8. SYSTEM ELEMENT
3	I-2 pages, II-1 page, III-3 pages		MGDS System Element
	Print Name	Signature	Date
9. Originator	John Massari	<i>John Massari</i>	4/14/95
10. Checker	LARRY HASSLER	<i>Larry Hassler</i> For Kevin McCoy	4/14/95
11. Lead Design Engineer	PETER GOTTLIEB	<i>Peter Gottlieb</i>	4/14/95
12. QA Manager	Joe Willis	<i>Joe Willis</i>	4-14-95
13. Department Manager	PETER GOTTLIEB (FOR H.A. BENTON)	<i>Peter Gottlieb</i> FOR H.A. BENTON	4-14-95
14. REMARKS			

Design Analysis Revision Record

Complete only applicable items.

①

2. DESIGN ANALYSIS TITLE		
Initial Waste Package Probabilistic Criticality Analysis: Uncanistered Fuel (TBV-059-WPD)		
3. DOCUMENT IDENTIFIER (Including Rev. No.)		4. REVISION NO.
B00000000-01717-2200-0079 REV 00		00
5. Revision No.	6. Total Pages	7. Description of Revision
00	61 + 3 Attachments 67 Total Pages	Original Issue

**INITIAL WASTE PACKAGE
PROBABILISTIC CRITICALITY
ANALYSIS: UNCANISTERED FUEL
(TBV-059-WPD) (SCPB: NIA)**

April 14, 1995

Originator: J.R. Massari

Checker: J.K. McCoy

Table of Contents:

<u>Item</u>	<u>Page</u>
1. Purpose	5
2. Quality Assurance	6
3. Method	6
4. Design Inputs	7
4.1 Design Parameters	7
4.2 Criteria	7
4.3 Assumptions	8
4.4 Codes and Standards	8
5. References	8
6. Use of Computer Software	11
7. Design Analysis	11
7.1 System Description	11
7.2 Failure Modes and Effects Analysis	14
7.3 Development of Fault Tree Logic	18
7.4 Development of Probabilities and Probability Density Functions (pdf) ...	21
7.4.1 Flow Defining Events	21
7.4.2 Concentration of flow on individual waste package	24
7.4.3 Corrosion Events	26
7.4.4 Probability of sufficient fissile material in a package	36
7.4.5 Evaluations of two-fold convolutions of pdfs	37
7.4.6 Probability of sufficient moderator	39
7.4.7 Probability that fuel assemblies maintain geometry required for criticality	39
7.5 Fault Tree Analysis	54
8. Conclusions	60
9. Attachments	61

1. Purpose

This analysis is prepared by the Mined Geologic Disposal System (MGDS) Waste Package Development Department (WPDD) to provide an assessment of the present waste package design from a criticality risk standpoint. The specific objectives of this initial analysis are to:

1. Establish a process for determining the probability of waste package criticality as a function of time (in terms of a cumulative distribution function, probability distribution function, or expected number of criticalities in a specified time interval) for various waste package concepts;
2. Use the established process to estimate the probability of criticality as a function of time since emplacement for the uncanistered fuel waste package (UCF-WP);
3. Identify the dominant sequences leading to waste package criticality for subsequent detailed analysis.

The purpose of this analysis is to document and demonstrate the developed process as it has been applied to the UCF-WP.

Due to the current lack of knowledge in a number of areas, every attempt has been made to ensure that the all calculations and assumptions were conservative. This analysis is preliminary in nature, and is intended to be superseded by at least two more versions prior to license application. In this sense, all of the results and information contained herein are TBV. The final output of this document, the probability of UCF-WP criticality as a function of time, has been assigned TBV identifier number TBV-059-WPD. Future versions of this analysis will update these results, possibly replacing the TBV with a small number of TBV's on individual items, with the goal of removing all TBV designations by license application submittal.

This document is intended to deal only with the risk of internal criticality with unaltered fuel configurations. The risk of altered fuel configuration, or external, criticalities will be evaluated as part of our ongoing criticality risk analyses. The results will be contained in interim reports, and collected into the next version of the Waste Package Probabilistic Criticality Analysis (1996).

Originator: J.R. Massari	Checker: J.K. McCoy
---------------------------------	----------------------------

2. Quality Assurance

This activity entails the use of risk assessment techniques to assess the probability of a UCF-WP criticality event. This activity will also provide input for the Total System Performance Assessment (TSPA) which will be included in the License Application Design (LAD) phase and may be used to set design requirements and material specifications. Therefore, it has the potential to affect the design and fabrication requirements of the Waste Package/Engineered Barrier Segment. This activity can impact the proper functioning of the MGDS waste package; the waste package has been identified as an MGDS Q-List item important to safety^(5.1). The QA Program applies to this analysis. A QAP-2-3 evaluation has not been performed for the MGDS waste package (TBD-155). The WPDD QAP-2-0 Work Control evaluation^(5.2) determined that Activity Number 2.4.6 "Perform Waste Package Risk Analysis," within which this analysis is prepared, is subject to QARD requirements^(5.3). The information and results presented in this analysis are preliminary and, at this time, are yet to be verified (TBV-059-WPD). Any additional notation of TBV will be omitted since the TBV qualification applies universally to the contents of this analysis.

3. Method

A quantitative estimate of the probability of a UCF-WP criticality event, and the dominant sequences leading to this event, will be determined using the method of fault tree analysis. In the first step, a qualitative Failure Modes and Effects Analysis (FMEA) will be performed to determine the credible initiating events, and UCF-WP failure modes which could lead to criticality. This process is similar to that used for failure mode analysis of complex systems, such as those in a nuclear power plant. In the present case the system is the engineered barrier (whose components include the barriers and basket of the waste package). Failure modes for components within the defined system are evaluated for their impact on other components and the system as a whole.

The FMEA will be conducted within the framework of a fault tree analysis. The analysis method includes the following steps:

1. Definition of the system to be analyzed and its boundaries;
2. Performance of a qualitative Failure Modes and Effects Analysis (FMEA) to determine the credible initiating events and subsequent individual component failure modes (basic events) which could lead to criticality;
3. Development of the fault tree logic structure indicating the sequences of events which could lead to waste package criticality (the top event);
4. Description of discrete events and those which take place continuously over time;

Originator: J.R. Massari	Checker: J.K. McCoy
---------------------------------	----------------------------

5. Estimation of probabilities of discrete events and probability density functions (probabilities per unit time) based on the current understanding of their likelihood of occurrence;
6. Quantification of the fault tree to determine the probability of occurrence of the top event (waste package criticality).

Initiating and basic event probabilities used in the fault tree will be determined by statistical analysis of experimental information on UCF-WP material degradation, with the assistance of empirical, mathematical models of underlying physical mechanisms and forecasts of the environmental conditions and hazards which make up the initiating events.

4. Design Inputs

4.1 Design Parameters

Waste Package

Maximum UCF-WP Outer Length: 5642 mm, Reference 5.5
Outer Barrier Material: ASTM A 516 Carbon Steel, Reference 5.5
Outer Barrier Thickness: 100 mm, Reference 5.7
Inner Barrier Material: Incoloy Alloy 825, Reference 5.5
Inner Barrier Thickness: 20 mm, Reference 5.7
Basket Absorber Material: Borated Type 316 Stainless Steel Reference 5.7
Filler Material: Inert Gas, Reference 5.7

Emplacement Drift and Near-field Environment

Thermal Loading: 24.2 MTU/acre Reference 5.11
Backfill: None, Reference 5.5
Drift Diameter: 4.27 m (14 ft), Reference 5.11
TSw2 Volumetric Fracture Freq.: 19.64 fractures/m³ Reference 5.24

4.2 Criteria

The analysis addresses the probability of criticality events. Such work is a partial response to the following requirements:

The Engineered Barrier Segment design organization shall establish and execute a reliability, availability, and maintainability program to support Integrated Logistics Support and the general engineering program for the Engineered Barrier Segment. Reliability shall be addressed as an element of design reviews. [EBDRD 3.2.5.1.1]^(5.4)

The Engineered Barrier Segment shall be designed to ensure that a nuclear criticality accident is not possible unless at least two unlikely, independent, and concurrent or sequential changes have occurred in the conditions essential to nuclear criticality safety. Each system shall be designed for criticality safety under normal and accident conditions.

Originator: J.R. Massari	Checker: J.K. McCoy
---------------------------------	----------------------------

The calculated effective multiplication factor must be sufficiently below unity to show at least a five percent margin, after allowance for the bias in the method of calculation and the uncertainty in the experiments used to validate the method of calculation. [EBDRD 3.2.2.6.A]^(5.4)

4.3 Assumptions

Assumptions and their bases are given in Section 7, in connection with the individual events. They have been italicized for easy identification. The assumptions are generally conservative, so that they involve larger probabilities of the events in the sequences leading to criticality. The only exception is for the corrosion events, for which we have attempted to be as realistic as possible, within the context of presently available experimental and theoretical understanding.

4.4 Codes and Standards

The following document was used as a standard for the construction and evaluation of fault tree models:

Fault Tree Handbook, NUREG-0492, U.S. Nuclear Regulatory Commission, Washington, D.C., January 1981^{5,6}

5. References

- 5.1 "Yucca Mountain Site Characterization Project Q-List," YMP/90-55Q, REV 3, December 1994
- 5.2 "Evaluation of Waste Package Development Activities for Fiscal Year 1995," DI# BBA000000-01717-2200-00003 REV 01, February 24, 1995
- 5.3 "Quality Assurance Requirements and Description," DOE/RW-0333P, REV 1, July 21, 1994
- 5.4 "Engineered Barrier Design Requirements Document," YMP/CM-0024 REV 0, July 21, 1993
- 5.5 "Controlled Design Assumptions Document," DI# B00000000-01717-4600-00032 REV 00, August 29, 1994
- 5.6 "Fault Tree Handbook," NUREG-0492, U.S. Nuclear Regulatory Commission, Washington D.C., January 1981
- 5.7 "Initial Summary Report for Repository/Waste Package Advanced Conceptual Design," DI# B00000000-01717-5705-00015 REV 00, August 29, 1994

Originator: J.R. Massari	Checker: J.K. McCoy
---------------------------------	----------------------------

- 5.8 Modarres, M., "What Every Engineer Should Know About Reliability And Risk Analysis," Marcel Dekker, Inc., New York, NY, 1993
- 5.9 McCoy, J.K., "Corrosion Model For Corrosion-Allowance Materials," IOC LV.WP.JKM.8/94.201, August 5, 1994
- 5.10 Stahl, David, "Waste Package Corrosion Inputs," IOC LV.WP.DS.06/93.107, June 21, 1993
- 5.11 Bahney III, R.H., "Thermal Evaluations of Waste Package Emplacement," DI# BBA000000-01717-4200-00008 REV 00, July 21, 1994
- 5.12 Buscheck, T.A., Nitao, J.J, Saterilie, S.F., "Evaluation of Thermo-Hydrological Performance in Support of the Thermal Loading Systems Study," in *High Level Radioactive Waste Management: Proceedings of the Fifth International Conference*, (American Nuclear Society, La Grange Park, IL, and American Society of Civil engineers, New York, 1994), pp. 592-610
- 5.13 Sandia National Laboratories, "Total-System Performance Assessment for Yucca Mountain - SNL Second Iteration" (TSPA-1993) (SAND93-2674), April 1994
- 5.14 Knief, R.A., "Nuclear Criticality Safety - Theory and Practice," American Nuclear Society, La Grange Park, IL, 1993
- 5.15 "Initial Demonstration of the NRC's Capability to Conduct a Performance Assessment for a High-Level Waste Repository," NUREG-1327, May 1992
- 5.16 Gdowski, G.E., Bullen, D.B., "Survey of Degradation Modes of Candidate Materials for High-Level Radioactive- Waste Disposal Containers," UCID-21362 Vol. 2, August 1988
- 5.17 "Immersion Studies On Candidate Container Alloys For The Tuff Repository," NUREG/CR-5598, May 1991
- 5.18 "CRC Handbook Of Chemistry and Physics," 66th Edition, CRC Press, Inc., Boca Raton, FL, 1985
- 5.19 "Swedish Nuclear Fuel and Nuclear Waste Management Co, Site Characterization and Validation - Final Report," STRIPA PROJECT 92-22 (April 1992)
- 5.20 "ASM Handbook, Volume 13 - Corrosion," ASM International, December 1992

Originator: J.R. Massari	Checker: J.K. McCoy
---------------------------------	----------------------------

- 5.21 McCright, R.D., Halsey, W.G., Van Konynenburg, R.A., "Progress Report On The Results Of Testing Advanced Conceptual Design Metal Barrier Materials Under Relevant Environmental Conditions For A Tuff Repository," UCID-21044, December 1987
- 5.22 Jones, D.A., Howryla, R.S., "Electrochemical Sensor to Monitor Atmospheric Corrosion in Repository Environments," presented at Waste Package Workshop, Las Vegas, Nevada, September 21-23, 1993
- 5.23 "Pitting, Galvanic, and Long-Term Corrosion Studies on Candidate Container Alloys for the Tuff Repository," NUREG/CR-5709, January 1992
- 5.24 Bauer, S.J., Hardy, M.P., Lin M., "Fracture Analysis and Rock Quality Designation Estimation for the Yucca Mountain Site Characterization Project," SAND92-0449, February 1993
- 5.25 Gottlieb, P., "Waste Package Design Basis Fuel Analysis", DI# BBA0000000-01717-0200-00121 REV 00, February 22, 1994
- 5.26 Cerne, S.P., Hermann, O.W., and Westfall, R.M., "Reactivity and Isotopic Composition of Spent PWR Fuel as a Function of Initial Enrichment, Burnup, and Cooling Time", Oak Ridge National Laboratory, 1987 (ORNL/CSD/TM-244)
- 5.27 National Research Council, "Ground Water at Yucca Mountain, How High Can it Rise", National Academy Press, Washington, D.C., 1992
- 5.28 Andrews, R., Dale, T., and McNeish, J., "Total System Performance Assessment-1993: An Evaluation of the Potential Yucca Mountain Repository", DI# B00000000-01717-2200-00099 REV 01, 1994.
- 5.29 Flint, A.L., Flint, L.E., "Spatial Distribution of Potential Near Surface Moisture Flux at Yucca Mountain", Proceedings of the Fifth Annual International Conference on High Level Radioactive Waste Management, pp. 2352-2358, American Society of Civil Engineers, 1994
- 5.30 Anna, L., Private communication

Originator: J.R. Massari**Checker: J.K. McCoy**

6. Use of Computer Software

Lotus 1-2-3 Release 4.01 spreadsheet software was used to plot distributions and graphs, perform the convolution of water intrusion, waste package breach, and neutron absorber leach distributions, and as a general calculational aid. Plotting of the fault tree diagrams and quantification of the fault tree top event was performed using CAFTA version 2.3. In the process of fault tree display and quantification, CAFTA performs only simple arithmetic operations, similar to a spreadsheet. In this sense it can be classified as computational support software. The correctness of the software is evidenced by its industry-wide acceptance, and is independently verified by a spreadsheet in Attachment II.

7. Design Analysis

7.1 System Description

The first step in performing any risk analysis is to provide a clear and concise description of the boundaries of the system to be analyzed. The system boundary for this analysis includes the waste package and the local drift environment into which it has been emplaced (see Figure 7.1). These are collectively referred to as the engineered barrier system in the context of this analysis. Events which may affect the local drift environment but are not part of the system defined here, such as changes in water infiltration rate or climate, are considered external events (which are usually initiating events).

The waste package concept to be evaluated in this analysis is the 21 Pressurized Water Reactor (PWR) fuel assembly Uncanistered Fuel Waste Package (UCF-WP) described in section 6.2.3 of Reference 5.7. Criticality risk for the emplacement package containing the Multi-Purpose Canister (MPC) is evaluated in a companion document to this. Other spent fuel configurations will be included with the update of this analysis planned for April 1996. In the UCF-WP, spent nuclear fuel (SNF) assemblies are isolated from the external environment by a container consisting of two layers or barriers. The outer barrier consists of 100 mm of A 516 carbon steel corrosion allowance material. The inner barrier is fabricated from 20 mm of Incoloy Alloy 825 corrosion resistant material. Two designs have been proposed for the internal basket structure; an interlocking plate basket (ILB) design, and a bundled tube basket design. The ILB design provides criticality control by fabricating all plates separating fuel assemblies from neutron absorbing material. This material consists of 10 mm of borated Type 316 stainless steel. The tube design achieves criticality control by placing each assembly in neutron absorbing Type 316 borated stainless steel tubes that are 5 mm thick (resulting in 10 mm of borated stainless steel between adjacent assemblies). *For the current analysis, both designs will be treated identically as a single 10 mm thickness of stainless steel. The remainder of the interior of the UCF-WP is assumed to contain only an inert gas and no filler material^(5.7). The UCF-WP design is assumed to have a maximum external length of 5.642 m^(5.5).*

Originator: J.R. Massari	Checker: J.K. McCoy
--------------------------	---------------------

The local emplacement environment to be used in this evaluation is consistent with the horizontal in-drift emplacement concept using a low-thermal loading (24.2 MTU/acre) strategy and 4.27 m (14 ft) drifts. *It is also assumed that backfilling of the emplacement drifts has not been performed.* With a low thermal loading, the near-field temperatures fall below the boiling point of water within 200 years following last emplacement^(5.11). The lower temperatures result in reduced rock stresses, providing more stable and longer lived emplacement drift openings. However, the relatively quick drop below the boiling point of water (as opposed to that for a high thermal loading) greatly reduces the time before liquid water can come into contact with the waste package. The presence of water would result in more rapid corrosion of the waste package barriers and enhance the subsequent leaching of the neutron absorber material from the basket structure. It also allows for the possibility that the waste package interior could fill with water (which is the most efficient moderator available in the natural environment) immediately following breach of the outer and inner barriers, thus creating an environment for neutron moderation. Therefore, within the present understanding of the Yucca Mountain hydro-thermal processes, evaluating the UCF-WP with a low thermal load is a conservative assumption with respect to criticality. It should be noted that the recent CRWMS/M&O TSPA-93^(5.28) has shown the intermediate thermal loading (57 kw/acre) to be more stressing with respect to radionuclide release. If that alternative is under active consideration at the time of the next revision of this document (1996) then it will be included.

Originator: J.R. Massari	Checker: J.K. McCoy
---------------------------------	----------------------------

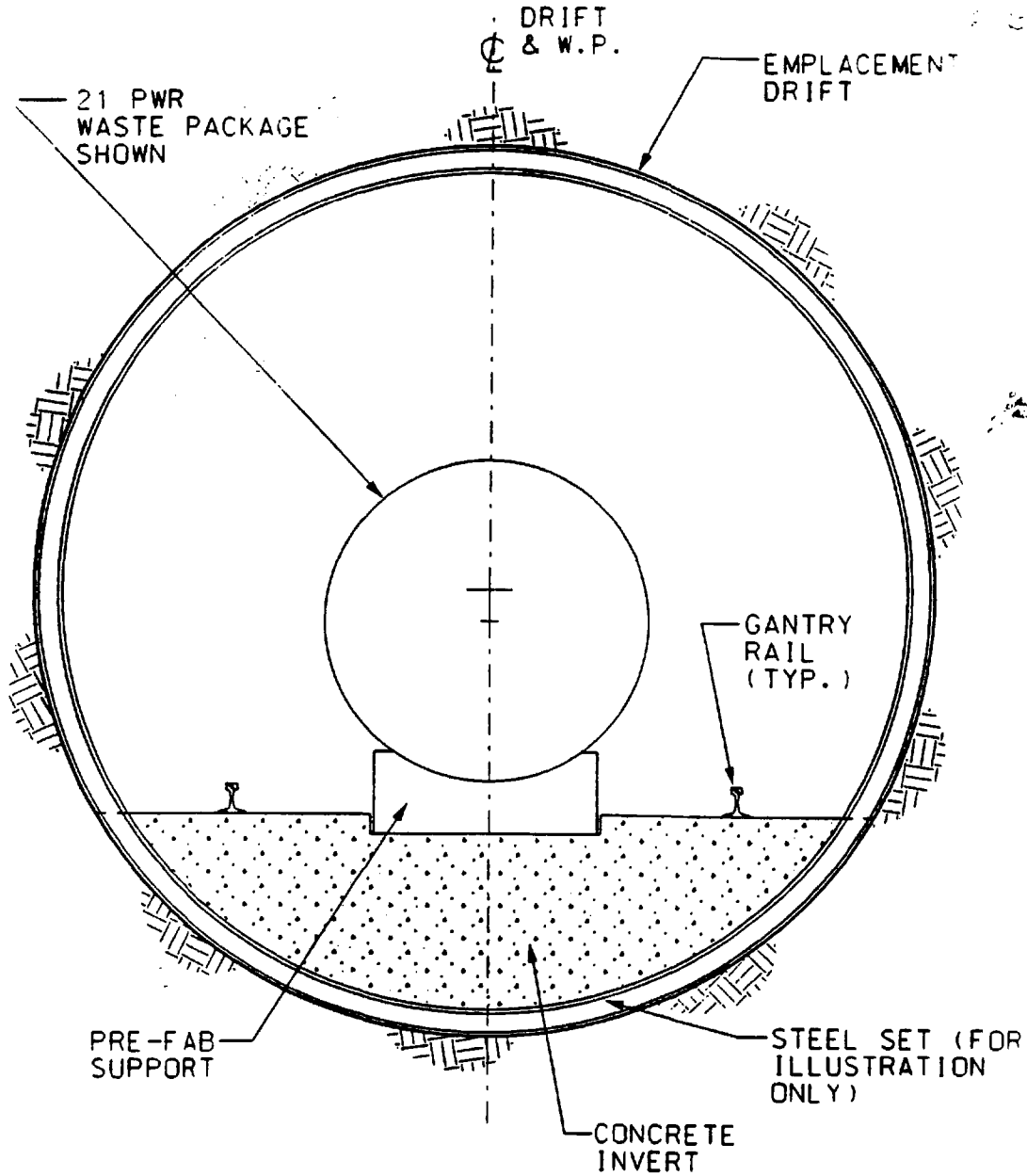


Figure 7.1. Waste Package and Local Drift Environment

Originator: J.R. Massari	Checker: J.K. McCoy
--------------------------	---------------------

7.2 Failure Modes and Effects Analysis

To assist in the development of the fault tree logic diagram, the technique of failure modes and effects analysis (FMEA) has been applied to the system of the waste package and its local drift environment. The FMEA process is qualitative in nature and is useful in determining sequences of events which can cause the defined system to fail to perform its intended function. The mission of the engineered barrier system being evaluated by this analysis is to safely contain fissile material and other radionuclides and isolate them from the accessible environment. In accomplishing the above mission, one of the functions performed by the system is to maintain the waste package in a subcritical condition. This is the function to be evaluated by this analysis, and the failure of the waste package to remain subcritical will represent the top event of the fault tree to be developed in Section 7.3. For the events in the more probable (but still unlikely) sequences leading to criticality, the probability of discrete events and probability density functions (pdf) for the events continuous in time will be developed in Section 7.4. These events can also be interpreted as engineered barrier system component failure modes, with their relationships provided in Table 7.1.

Event sequences leading to criticality

This analysis considers only water moderated criticality internal to the waste package. It has been shown that unmoderated criticality is impossible for intact light water reactor fuel with fissile content less than 5%^(5.14). Water is the only moderator present in the waste package environment which can enter the waste package. External criticality, which could involve moderation by silica, will be considered in the 1996 version of this analysis.

While a large list of event sequences (scenarios) involving extensive water intrusion has been proposed for performance analyses of radionuclide containment^(5.15) (i.e., magmatic intrusion, excavation by future drilling, etc.), most of these could not result in criticality. Only two basic scenarios are capable of introducing water into the local drift environment in a manner which could create the conditions necessary for a criticality event. These involve 1) the possible concentration of the episodic infiltration flux by a fracture directly over a waste package (hereafter referred to as the "concentration" scenario), and 2) the possible flooding of a drift due to an external event producing a significant rise in the water table (for which the principal mechanisms are changing of the climate to wetter conditions or a severe tectonic event) or high infiltration combined with poor drift drainage. These event sequences (scenarios) can be described in terms of the following specific events:

1. Concentration of the flow so as to directly impinge upon the waste package (e.g., flowing fractures in the drift directly above the waste package, or flooding of the entire drift). A fracture configuration leading to such concentration is assumed to be stable with respect to minor geologic changes over thousands of years, but not

Originator: J.R. Massari	Checker: J.K. McCoy
---------------------------------	----------------------------

- necessarily with respect to events on a 100,000 year time scale which could produce major geologic changes,
2. Increased water flow or flooding,
 3. Breach of the waste package to permit moderator entry (primarily by corrosion),
 4. Leach of the neutron absorber from the containing matrix,
 5. Ponding of water in the waste package to serve as a stable moderator (which is a direct consequence if the alternative flooding is used in steps 1 or 2 above), and
 6. All of the above events act on a package which has enough fissile material to go critical (SNF with high enough enrichment and low enough burnup).

The above water intrusion scenarios are conditional on the temperature of the rock in the local drift environment being below 100°C. The initiating events for this analysis are therefore defined as infiltration flow (nominal and high rates), flooding due to climate change, and flooding due to severe tectonic activity.

Component Failure Modes

Of the 6 events (or conditions) listed above as being essential ingredients of a criticality sequence (scenario), the third and fourth can be viewed as failure modes of individual components of the waste package: the barriers (inner and outer) component and the basket component.

Failure Modes of the Immediate Rock Environment

The repository is based on the assumption that the rock environment (including available moisture) will severely limit infiltrating water and prevent its coming into contact with the waste package. The presence of concentration fractures in the drift ceiling above a waste package which could direct infiltrating water onto a waste package represents one mode of failure of this environment. Another possible mode of failure is the collapse of a drift opening in such a way that a local dam is created, causing flooding of the drift if sufficient infiltration flow is available to the drift by the fractures described above. However, as mentioned previously, drift flooding can also occur in the absence a drift failure mode due to an initiating event which causes a rise in the water table to the repository horizon.

There are also several possible rock failure modes which could directly affect the integrity of the waste package. These include events which could impose a severe mechanical stress on the waste package, such as the impact of a falling rock or shearing by the movement of a new or unidentified fault. However, subsequent flooding of the drift and leaching of the neutron absorber would be required before a criticality event could occur. Such sequences are presently estimated to have small probability of occurrence and will not be represented in the fault tree diagram. Specific estimates of their probabilities and consequences will be included in future analyses.

Originator: J.R. Massari	Checker: J.K. McCoy
---------------------------------	----------------------------

Table 7.1. Summary of Engineered Barrier System Failure Modes and Criticality Effects

Component	Function	Failure Modes	Mechanisms	Effects	Comments
Immediate rock environment. (Surrounding the emplacement drift)	Provide an environment which ensures long waste package life by limiting contact with water and other hazards	Fails to prevent infiltrating water from contacting waste package	Hydraulically conductive ceiling fracture concentrates infiltrating water onto waste package	Eventual corrosion of barriers, and possible filling of WP, and leaching of neutron absorber.	Requires infiltration of surface water to initiate sequence. Requires proper corrosion hole configuration to fill WP.
			Drift collapse forms a dam, preventing drainage of infiltrating water from drift.	Eventual flooding of drift and immersion of one or more WPs. Eventual corrosion of barriers, filling of WP, and leaching of absorber.	Requires infiltration of surface water to initiate sequence. However, flooding may occur in the absence of drift failure modes due to other initiating events.
		Fails to prevent mechanical damage to waste package.	Rock fall or faulting incident on waste package, which may be partially degraded by corrosion.	Possible breach of WP barriers depending on amount of applied stress and degree of barrier degradation.	Sequence not included in current fault tree.

Table 7.1. Summary of Engineered Barrier System Failure Modes and Criticality Effects

Component	Function	Failure Modes	Mechanisms	Effects	Comments
Waste Package Barriers	Isolate SNF from environment and prevent intrusion of water to interior.	Waste package barriers breached, allowing moderator entry and neutron absorber removal.	Corrosion of barriers by intruding water.	WP eventually breached. Immediate filling under flooded conditions. Specific corrosion hole configuration required for filling by overhead dripping.	Rate of corrosion varies according to drift conditions. Rates of sufficient magnitude to cause breach in the time frame of this analysis are conditional on water intrusion.
			Pre-existing through-wall defect in both barriers	WP barriers breached. Immediate filling if flooded conditions occur.	Sequence not included in current fault tree.
Waste Package Basket	Maintain SNF in a subcritical condition	Insufficient neutron absorber available to maintain sub-criticality under moderated conditions	Sufficient neutron absorber leached from basket material by intruding water	Waste package criticality if fuel assemblies maintain appropriate geometry and basket filled with water.	Leaching is conditional on waste package breach and intrusion of water.
			Basket material doped with insufficient absorber during fabrication	WP criticality if fuel assemblies maintain proper geometry and basket filled with water.	Sequence not included in current fault tree.





7.3 Development of Fault Tree Logic

The fault tree approach is a deductive process whereby an undesirable event, called the top event, is postulated, and the possible means for this event to occur are systematically deduced. In this analysis, the undesired event is waste package criticality. In the previous section, the deductive FMEA process was performed to determine the basic criticality scenarios, initiating events, and engineered barrier system failure modes that could lead to a waste package criticality event. In this section, the results of the FMEA will be used to develop the fault tree logic diagram.

The fault tree diagram is a graphical representation of the various parallel and sequential combinations of faults that lead to the occurrence of the top event. The methodology and symbols used in the construction of the fault tree diagram are given in the Fault Tree Handbook^(5,6). Figure 7.2 is provided as a reference for the symbols utilized in this analysis. The fault tree developed from the engineered barrier system FMEA is shown in Figure 7.3. The fault tree was plotted using CAFTA version 2.3 fault tree analysis software. In addition to a one line description, each intermediate gate, basic event, and conditional event, is uniquely identified with an acronym. These acronyms will be used as identifiers for each gate and event in the quantification of the fault tree that is performed in Section 7.5. These acronyms are individually identified with the complete event descriptions in the headings of the subsections of Section 7.4, where we have also given the derivation of the associated probabilities and probability density functions.

Originator: J.R. Massari	Checker: J.K. McCoy
---------------------------------	----------------------------

PRIMARY EVENT SYMBOLS

-  **BASIC EVENT** – A basic initiating fault requiring no further development
-  **CONDITIONING EVENT** – Specific conditions or restrictions that apply to any logic gate (used primarily with PRIORITY AND and INHIBIT gates)
-  **UNDEVELOPED EVENT** – An event which is not further developed either because it is of insufficient consequence or because information is unavailable
-  **EXTERNAL EVENT** – An event which is normally expected to occur

GATE SYMBOLS




-  **AND** – Output fault occurs if all of the input faults occur
-  **OR** – Output fault occurs if at least one of the input faults occurs
-  **INHIBIT** – Output fault occurs if the (single) input fault occurs in the presence of an enabling condition (the enabling condition is represented by a CONDITIONING EVENT drawn to the right of the gate)

Figure 7.2. Definitions of Event and Gate Symbols Used in Analysis

Originator: J.R. Massari	Checker: J.K. McCoy
---------------------------------	----------------------------

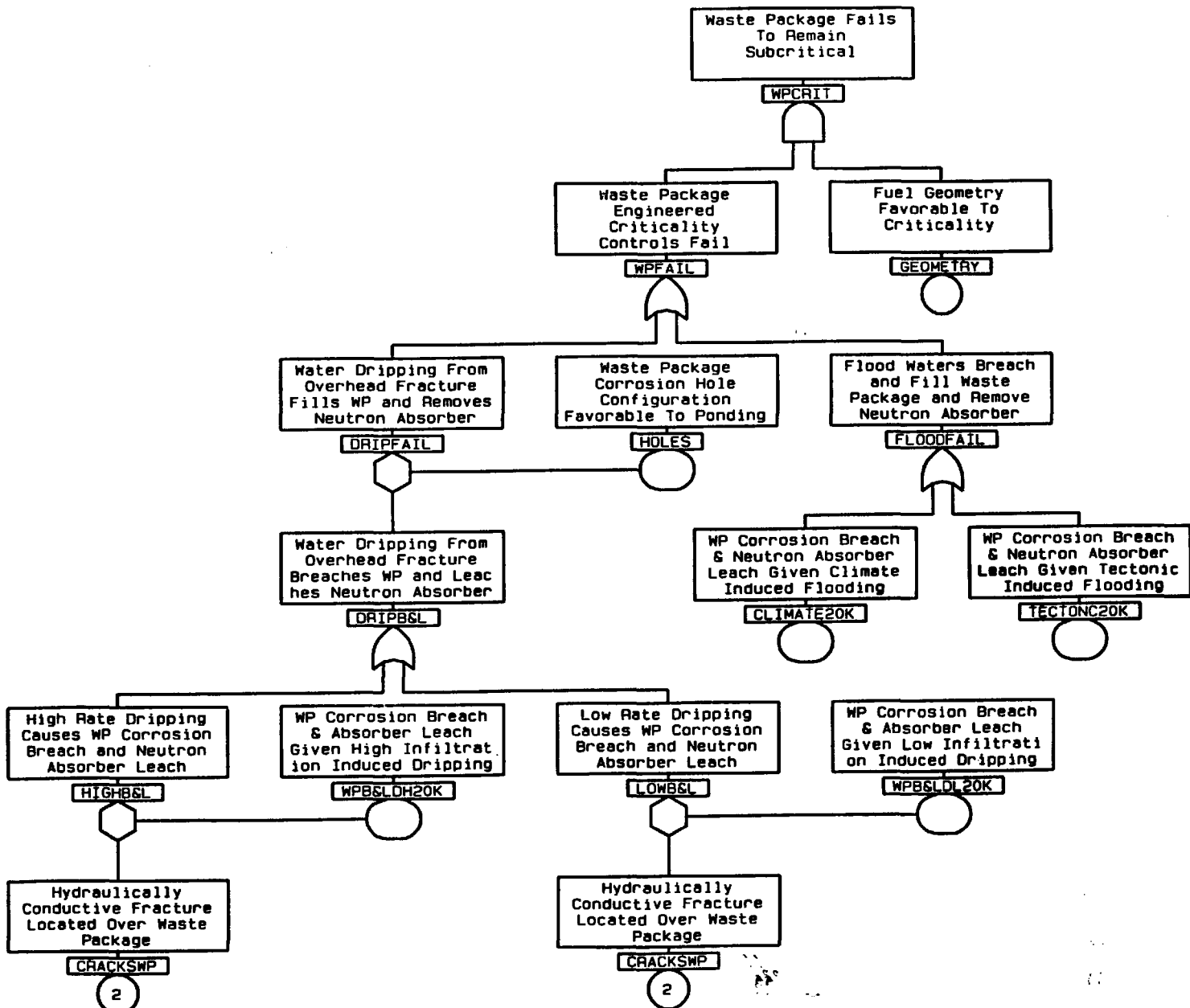


Figure 7.3. Initial Post-Closure Waste Package Criticality Fault Tree

Originator: J.R. Massari

Checker: J.K. McCoy

7.4 Development of Probabilities and Probability Density Functions (pdf)

The following sections provide a detailed description of the estimation of the probabilities of discrete events and the probability density function of events which are continuous in time. All basic, conditional, and initiating events in the fault tree diagram for the system defined in Section 7.1. Event identifiers used to abbreviate the full description in the analysis of the fault tree are given in parentheses. Event probabilities and pdf's have been summarized in Table 7.5.

The three events involving water: (1) flow defining events (increased flow or repository flooding), (2) breach of the waste package by aqueous corrosion, (3) leach of the absorber by dissolution of the basket, will be represented by pdf's which will be convolved together to incorporate the fact that they must occur in the sequence indicated. In other words, the pdf for the occurrence of all three events, with the last event occurring at time t , requires that event 1 take place at some time, $0 < t_1 < t$, followed by event 2 at some time $t_1 + t_2$, such that $0 < t_1 + t_2 < t$, which is followed by event 3 occurring at time t . The pdf for t is then found from the two-fold convolution

$$f(t) = \int_0^t f_1(t_1) dt_1 \int_0^{t-t_1} f_2(t_2) f_3(t-t_1-t_2) dt_2 \quad (1)$$

7.4.1 Flow Defining Events

These are the initiating events; all are characterized by a pdf, denoted by $f_1(t)$. All describe a state of flow or flooding; *it is assumed that this state continues indefinitely once initiated*. In other words, we use a pdf to define the probability of occurrence within a small interval of time centered about a specific time and assume that the occurred condition will continue indefinitely. This is a very conservative assumption, since it is possible that any increased state of flow or flood will eventually revert to something like the original state before the enhanced corrosion rate has completed the corrosion of the waste package component (barrier or basket). These pdf's are all in expressed in units of per-year.

It should be noted that the description of alternative flow defining events is intended to be qualitative only, without specifying the actual water accumulation (net of infiltration and outflow). The effects of these flows are treated more quantitatively in section 7.4.3 (Corrosion Events) below.

The events, or event scenarios, described below reflect alternative forecasts of climatological or tectonic change. As such they should be mutually exclusive. However, this would be an oversimplification. The actual environmental changes over the next 1,000,000 years would be a mixture of these four alternatives at different points in time. An analysis based on comparison of the large number of combinations possible would be confusing and difficult to interpret, and, considering the uncertainty in the forecast process itself,

would not be very meaningful. For these reasons we have calculated the pdf's as if each event were certain to occur, given enough time. The question of how to combine these probabilities does not arise until we have convolved them with the corrosion breach and leach pdf's and with the discrete probabilities for sufficient fissile material and sufficient moderator (sections 7.4.4 and 7.4.6, below).

Pdf for Surface water infiltration of repository horizon at a low rate (f_1 for wpb&ldl)

This is the probability that a corrosively significant stream will pass through the waste emplacement areas. Such a stream would have to accumulate sufficient volume to fill a waste package to a depth of at least 1 meter. Over a period of 10000 years, this would require a flow rate of 0.1 mm/yr, which just happens to be the middle of the flow rate range presently estimated for the repository area^(5,29). However, in addition to ponding in the package, there must be enough flow to leach out the boron absorber from the basket; *we conservatively estimate that at least a factor of 10 increase would be required for such a process*, for a total infiltration rate of 1 mm/yr. [Note: This estimation of required flow rate is only to define this low infiltration category. The actual rate of basket leach is estimated in section 7.4.3.2 (Corrosive leach of absorber/basket) below.] For such an increased flow rate to be maintained over many years, there would have to be a significant climate change (one as significant as an ice age). *We very conservatively estimate that such an event is certain to occur within 10,000 years (and that such an enhanced flow rate would be maintained thereafter)*. It should also be more likely at the end of this period than at the beginning, since such a changed climate would take thousands of years to develop. Nevertheless, we chose a conservative probability model, the uniform distribution between 1000 and 10000 years, which can be expressed in units of per year as

$$f_1(t) = 1/9000 \quad 1000 < t < 10000 \quad (2)$$

This pdf is shown in Figure 7.4, together with the resulting cdf.

Pdf for surface water infiltration of repository horizon at a high rate (f_1 for wpb&ldh)

This would be an infiltration flow rate of greater than 10 mm/year, which is 10 times the low infiltration flow rate given above, and would be expected to give a correspondingly increased corrosion rate (on the waste package) and leach rate (for the boron). [It may be that 10 mm/yr is still so low as to not significantly disturb the corrosion passivating film, so that the conditional corrosion rate is not significantly higher than for low infiltration, but the boron leach rate would still be higher.] *Such a high infiltration rate would require a very significant climate change, which we estimate to be likely sometime between 2,000 years and 100,000 years (which would be likely to encompass several ice ages, and their aftermaths, which could result in increased atmospheric precipitation)*. As with the low infiltration case, we use the conservative uniform distribution, again expressed in units of per year

Originator: J.R. Massari

Checker: J.K. McCoy

$$f_1(t) = 1/98000 \quad 2000 < t < 100000 \quad (3)$$

This pdf, together with the associated cdf, is shown in Figure 7.5.

Change to a very wet climate raises water table to repository horizon (f_1 for climate)

The present tectonic trends are moving the climate in a dryer direction. For example, one major cause of the shift from a moist climate to a dry one over the past several million years has been the rise of the Sierra Nevada, which prevent the moist Pacific air from reaching Nevada. Flooding of the repository would require a substantial increase in rainfall, sustained over a long time period, since the proposed repository horizon is approximately 300 meters above the current water table. The National Research Council has examined the possibility of water table rise to the level of the repository^(5,27). They reported that even a 100% increase in rainfall (and a corresponding 15 fold increase in recharge) would produce an insufficient rise (raising the level only 150 meters). Their report also indicated that the last ice age saw only a 40% increase in precipitation (p. 6), and that as far back as 50,000 years ago the water table in the recharge area north of Yucca Mountain was no more than 100 meters above its present level (p. 78).

Therefore, we assume the probability of flooding due to climate change in the next 10,000 years to be zero. The probability of flooding thereafter is *conservatively* estimated from available geologic information. The National Research Council report cited above suggests that the return period for simple flooding to be greater than 10^6 years, and that the probability of flooding during the early part of this period is much less than later. This inequality is so small that *we can conservatively use an asymmetric triangular distribution with the upper limit at 10,000,000 years, which would be*

$$f_1(t) = 2 \times 10^{-14} t \quad 10,000 < t < 10,000,000 \quad (4)$$

where t is expressed in years, and f_1 is expressed in units of per year. For simplicity, we have normalized this pdf as if the lower limit were 0, instead of 10,000. This normalization approximation is valid to six significant figures, which is certainly adequate for this analysis. This pdf, together with the associated cdf, is shown in Figure 7.6.

A flood of the magnitude described above would affect all packages in the repository equally. This situation is commonly referred to as a non-lethal shock common cause failure in component reliability analysis^(5,8). Given a repository wide non-lethal shock, such as flooding and immersion of all waste packages, each waste package will fail independently with a conditional probability of p (to be defined later; see section 7.4.3.1). Therefore, the above flooding event frequency may be applied to any given package. This is appropriate since the fault tree top event will be in terms of a frequency of criticality per package which can then be multiplied by the number of packages to get the expected number of criticalities in the repository.

Pdf for severe tectonic activity raising water table to repository horizon (f_1 for tectonic)

Flooding can also be caused by hydrothermal or volcanic activity raising the water table from below. This would require a tectonic change comparable to the major volcanic activity which produced Yucca Mountain in the first place. The geologic record indicates that this has not happened for the last 10^7 years. *The time scale for occurrence of this severe tectonic activity is, therefore, similar to that which applies to climate change induced flood, so the pdf for this event will be assumed to be the same as that given in Figure 7.6.*

This reasoning is more conservative than the authoritative finding that the possibility of a dike intrusion close to the repository is less than 10^{-8} per year and would cause only a 10-15 meter rise in the water table anyway ^(5.27, p. 7). One possible type of seismo-tectonic event which has been advanced as a possible initiator of repository flooding is a rupture in the low permeability zone imputed to be the source of the steep hydraulic gradient north of the site. An authoritative analysis has shown that should such a barrier exist, its removal would cause no more than a 40 meter rise in the water table at the repository site ^(5.27, p. 70).

The conditions that occur as a result of tectonically induced flooding are similar in nature to those of the climatologically induced flooding. Therefore, this event can also be thought of in terms of a non-lethal shock leading to common cause failure of waste packages, and can be applied on an individual package basis as well.

A seismo-tectonic event could release perched water if it were present in any volume, but any subsequent flooding of the repository would be transient only, unless all possible avenues of repository drainage were blocked, a very unlikely event.

7.4.2 Concentration of flow on individual waste package

In order to be effective in corroding a hole in the package, the nominal infiltration flow must be concentrated over some localized position on the package (typically by the location of a flowing fracture). This localized flow serves both to generate the corrosion hole and to channel the water into that hole, from where it can fill the lower half of the package and leach the neutron absorber. This section estimates the probability that a rock fracture capable of concentrating the infiltrating water exists over the waste package and directs the flow onto the waste package (crackswp). *This probability is assumed to be a property of the repository which remains constant over at least 100,000 years during which we are concerned about corrosion from leaking of fractures on a waste package.* It has been suggested that fractures may be a dynamic occurrence over the time periods of interest, and that they may even increase with time. The mechanisms which have been proposed include (1) changing stress patterns (e.g., those caused by the time and/or spatial variations of the repository thermal load, including the local stresses from individual waste packages), and/or (2) diversion to alternate fractures from flowing fractures which

Originator: J.R. Massari

Checker: J.K. McCoy

might get plugged by some silica redistribution mechanism. However, there is no evidence that new, or alternate, fractures would possess the necessary connectivity to provide flow enhancement. Furthermore, there is no model of the hypothesized time dependent behavior, so a constant value intended to have a safety margin large enough to accommodate any increase with time of the number flowing fractures will be used. This probability will be expressed in units of per-package.

The first step in developing a probability that a waste package is located under a dripping fracture is to determine the frequency of these fractures per unit length of drift ceiling. We have started with an estimate of the non-directional volumetric fracture frequency for the TSw2 unit of approximately 19 fractures per m³, from available borehole sample data^(5,24). The present, simple, model does not account for more detailed parameters, such as distribution of aperture sizes or fracture surface conditions; such information will be incorporated into future models when it becomes available.

For the purposes of this analysis, the most appropriate form is a linear ceiling fracture frequency, which can be developed from the volumetric frequency. To do this, the above volumetric frequency was used to determine the number of fractures in a cylindrical volume of rock equivalent to a 1 m long section of a 4.27 m (14 ft) diameter emplacement drift (281 fractures). *It was then assumed that only 50% of the fractures would intersect the surface of the volume (evenly distributed) and that the drift ceiling constituted approximately 8% of the surface area of that volume (top 90° arc of drift).* This resulted in an estimate of approximate 11 fractures per meter of drift ceiling.

With the linear ceiling fracture frequency estimated, the next step is to determine the percentage of fractures capable of conducting and concentrating the infiltration flow. A study performed in the STRIPA validation drift found that 14% of the tunnel surface area accounted for nearly all the flowing fractures^(5,19, p. 139). The high flowing 14% actually had a three times higher fracture density, suggesting that such areas could be easily detected and avoided. Without more data on the variable density of fractures in the repository horizon, and some possible correlation of such data with any flowing water, we take a somewhat different approach.

We assume that there will be some density of undetected flowing fractures. *We estimate such a density by starting with the STRIPA 14% and applying it on a fracture basis rather than an area basis.* This may not seem conservative since the STRIPA flowing area has a higher density of fractures than the rest of the drift, but is conservative since we take no credit for detecting any of these high flow zones before emplacement. *Since the tuff at the repository horizon is unsaturated, and infiltrating water will be preferentially absorbed in the rock pores rather than flowing through fractures, we estimate that this flowing fraction of all fractures should be reduced by a factor of 100 for a drift in the TSw2 rock unit.* [Note: This is the most significant of the assumptions to be verified by the time of the next revision of this document.] With this assumption, the linear frequency of flowing/dripping ceiling fractures is estimated to be of 0.0157 fractures per

Originator: J.R. Massari	Checker: J.K. McCoy
---------------------------------	----------------------------

meter of drift ceiling or 1 flowing fracture every 64 meters. This frequency will have to be verified by actual observation in the Exploratory Studies Facility.

Lacking precise characteristics of the fracture flows in the repository horizon, this model is necessarily somewhat arbitrary. It will be revised in the next version of this document, according to ESF measurements expected by that time. In the meantime we can have some confidence in the model because it is consistent with the flowing fracture density in the "weeps model" developed by Sandia^(5.13, Ch.15). Furthermore, this result is somewhat consistent with the interim results of fracture mapping in the starter tunnel, which indicates 1 fracture per meter of drift, without restriction to ceiling, but only reduces that fraction slightly in order to specify connected fractures.^(5.30) This strong connectivity is expected to be reduced as the tunnel reaches further under the surface, and there should be some additional reduction in order to specify flowing fractures.

With the above estimate of the linear flowing fracture frequency, the probability that a certain number of flowing fractures, n , will be located in a given length of drift can be determined using a Poisson distribution,

$$Pr(n) = \frac{(\lambda x)^n \exp(-\lambda x)}{n!} \quad \text{for } x\lambda > 0, x=0,1,2,\dots \quad (5)$$

where λ represents the frequency of flowing fractures per unit drift length, x is the length along the drift in question. Given the above flowing fracture frequency, and a waste package length of 5.642 m, the probability that a waste package *does not* have a flowing fracture over it, $Pr(0)$, is 0.915. Therefore, the probability that a waste package has at least one flowing fracture over it is $1-Pr(0)$, or 0.085.

7.4.3 Corrosion Events

In this analysis, criticality cannot occur until the waste package barriers have been breached by corrosion and the basket material containing the neutron absorber has been leached. These corrosion processes will be represented by the pdf's f_2 and f_3 in the two-fold convolution given in section 7.4. This section describes the methodology for obtaining these pdf's.

At the present time there is a great range in the corrosion rates derived from the accepted experimental data. There is no definitive model to explain even a major portion of this data. For this reason, we have developed a probabilistic model which reflects the wide variation of observations with probability distributions for failure times of the individual components being corroded. In the present state of uncertainty regarding corrosion models, we have chosen to be realistic rather than conservative. To compensate for this lack of conservatism we have provided a complete alternative calculation under the worst case barrier corrosion assumption: that the outer and inner barriers are penetrated by pitting corrosion in no time at all following occurrence of the initiating event. This approach does not resolve the conflict between pitting and bulk corrosion interpretations

of some of the data, but it does present the range of possible consequences.

It is well known that rate of corrosion depends on many properties of the aqueous environment, particularly pH, which is incorporated into corrosion models more sophisticated than the model used here. However, most of the data comes from tests which were not controlled for these parameters, so we have chosen to use the experimental data in a model which reflects the worst case parameter values likely to be encountered in the aqueous environment. We have also simplified the analysis by neglecting dry oxidation since, (1) if water is present for any significant fraction of the time, dry oxidation will have a small effect by comparison, and (2) if water is never present we can't have an internal criticality.

For this analysis, *it has been assumed that the primary variables influencing the rate of corrosion in the postulated environments are the surface temperature of the waste packages and the chemistry of the intruding water. However, the latter will be postulated to be constant for a given environment unless otherwise stated.* The variations in waste package surface temperature with respect to time and location in the repository, provides the basis for the use of a pdf to represent time to breach of a given barrier.

Stahl^(5,10) has summarized diversity of measurements and analytic models with the following time and temperature dependent equation as a heuristic representation of the penetration of certain metals by aqueous corrosion,

$$P = At^c \exp\left(-\frac{B}{T}\right), \quad (6)$$

where P is corrosion penetration depth, t is time (years), T is temperature (K), and A , B , and c are constants. This equation is representative of experimental data for moderate temperatures (up to about 350°K). At higher temperatures the equation is expected to be conservative because it does not account for the decreasing solubility of oxygen. The value of c describes the degree of protection afforded the base metal surface by the corrosion products. For $c = 1$, the corrosion rate is independent of time if temperature and humidity are constant; this is appropriate if the products of corrosion are entirely unprotective. For $c = 0.5$, corrosion has the parabolic dependence on time that is typical for a layer of corrosion products that act as a diffusional barrier to corrosive species. Intermediate values of c can be used to describe varying degrees of protectiveness.

Stahl's formula is adequate for predicting aqueous corrosion penetration of a material that is held at constant temperature. However, because waste package surface temperatures will be time and location dependent, it becomes necessary to put Stahl's model into a form that gives the rate of corrosion. Since the definition of zero time is arbitrary, it is also desirable to have an expression for the corrosion rate that does not have an explicit time dependence. McCoy^(5,9) has proposed the following expression for corrosion rate, in which all time dependence is implicit:

$$dP/dt = \alpha P^\beta \exp(\gamma h(t) - \delta / T(t)) \quad (7)$$

Here h is a complement to the relative humidity H , and given by the expression $h = H(\text{in } \%) - 100$, and the remaining constants are as follows: α is a rate constant, β describes the protectiveness of the corrosion products, γ describes the humidity dependence, and δ describes the thermal activation. Equation 7 provides an expression for the corrosion rate that depends only on the amount of corrosion product present and the environmental conditions. The equation generalizes Stahl's equation in two ways: it is applicable to time-dependent environmental conditions, and it postulates a humidity dependence. By rearranging Equation 7 slightly and renaming the variables for consistency with Stahl's equation, one obtains

$$P = A \left(\int_0^t \exp[kh(t')/c - B/(cT(t'))] dt' \right)^c, \quad (8)$$

where k now describes the humidity dependence, and the correspondence of the other parameters is as follows;

$$c = 1/(1-\beta) \quad A = \alpha^c \quad B = \delta c.$$

A value of k , 0.1908 for a static environment, was obtained from measurements by Jones^(5.22) of corrosion current as a function of humidity. *Since McCoy's model is being used here to develop a failure distribution for a waste package in a flooded drift, the relative humidity will be taken to be 100% for all times when $T < 100^\circ\text{C}$ (the expression kh/c in the above formula will go to zero). This will simulate wetting of the waste packages as soon as physically possible after emplacement in a low thermally-loaded repository. This is a conservative assumption because (1) the repository temperatures (and thus the corrosion rates) may be substantially lower by the time an initiating event actually occurs, and (2) the actual boiling point of water at the repository horizon is $\approx 96^\circ\text{C}$. For times when $T \geq 100^\circ\text{C}$ the environment is taken to be a mixture of superheated steam and air at atmospheric pressure.*

For early years the waste package surface temperature depends primarily on its own internal heat and is best determined by a drift-scale calculation; for later years it depends on the average heat from all the packages and is best determined by a repository scale calculation. For the low thermal loading case, the dividing point is approximately 100 years after emplacement. For times less than 100 years the results of a waste package model developed by Bahney^(5.11) were used. Bahney created a three-dimensional finite element ANSYS model of near field and surface temperatures for a single waste package, with the remainder of the repository represented as an infinite grid of waste packages with 16 m along the drift between waste packages and 95 m between drifts. For times greater than 100 years, modified versions of the repository scale results of Buscheck^(5.12) were used. Buscheck calculated repository horizon temperatures for a disk-shaped repository with a smeared heat source. The difference in temperature between the waste package

Originator: J.R. Massari	Checker: J.K. McCoy
--------------------------	---------------------

surface and the repository horizon was calculated according to a correlation developed by McCoy^(5.9). That temperature drop was then scaled so that the temperature history would be continuous with Bahney's results at 100 years after emplacement. The resulting blended temperature history is shown in Figure 7.7. The various curves represent time-temperature profiles at different locations in the repository; percentages give the fraction of waste packages that are closer to the center of the repository than the package in question (0% is at the center, 25% is halfway from center to edge, and 100% is the edge).

For the functional form of the pdf for corrosion (f_2 or f_3) we will use the three parameter Weibull distribution, which is often used in reliability analysis to model corrosion resistance^(5.8). The pdf of the Weibull distribution is given by,

$$f(t) = \frac{\beta}{\alpha} \left(\frac{t-\theta}{\alpha}\right)^{\beta-1} \exp\left[-\left(\frac{t-\theta}{\alpha}\right)^\beta\right] \quad (9)$$

where α , β , and θ represent the scale, shape, and location parameters respectively (all > 0) and $t \geq \theta$. The associated Weibull cdf is given by,

$$F(t) = 1 - \exp\left[-\left(\frac{t-\theta}{\alpha}\right)^\beta\right] \quad (10)$$

for $t \geq \theta$. For values of $t < \theta$, both $f(t)$ and $F(t)$ equal zero. The values for α , β , and θ are typically chosen such that the shape of the resulting distribution closely matches the distribution of observed time to failure data of a sample of components.

7.4.3.1 Corrosive breach of waste package barriers

The first step in developing breach distributions was to determine values for the parameters required by McCoy's model. For aqueous general corrosion of carbon steel Stahl^(5.10) recommends $A=2525$ mm/yr, $B=2850^\circ\text{K}$ and $c=0.47$. Stahl indicates that these values are based on corrosion tests of cast steel and iron in seawater. The ASM Handbook^(5.20) also presents the results of a 9 week corrosion testing program performed for carbon steel in tuff groundwater at temperatures ranging from 50 to 100°C. Pitting corrosion rates were found to be approximately 1 mm/yr for most temperatures in the above range. Using Stahl's values for A and B, and assuming a c of 0.75, produces an average corrosion rate at 9 weeks time similar to that reported in the ASM Handbook. *Therefore, this analysis will assume a c of 0.75 for carbon steel.* This modification of c is considered appropriate, as the oxide layer formed during corrosion of carbon steel (i.e., rust) is typically regarded as providing very little protection against a corrosive environment.

The parameters for Alloy 825 were developed from available corrosion data for representative environments and assumptions about the time and temperature dependence of the material. *The temperature dependance parameter, B, was assumed to have a value of 5000°K, which is almost twice the value used for carbon steel.* This assumption was

Originator: J.R. Massari

Checker: J.K. McCoy

considered appropriate for a corrosion resistant material such as Alloy 825, as it typically maintains this resistance over a larger temperature range than carbon steel. *The protectiveness of the corrosion product layer was conservatively assumed to be similar to that of carbon steel, and thus, a c of 0.75 was chosen.* One source of corrosion data^(5.16) indicated that Alloy 825 experienced a corrosion rate 1.01 $\mu\text{m}/\text{yr}$ during 1.06 years of exposure to seawater at the ocean surface (temperature not given but assumed to be $\approx 27^\circ\text{C}$). The same source also indicated that this material experienced a corrosion rate of 1.86 $\mu\text{m}/\text{yr}$ during 1.13 years of exposure to a 566°C superheated steam environment. Using the values of B and c as given above, the superheated steam environment gives an A of 32664 mm/yr and the seawater gives an A of 16733 mm/yr . Another study sponsored by the Nuclear Regulatory Commission^(5.23) tested the corrosion behavior of Alloy 825 immersed in a sample of J-13 well water that was specifically modified to present an aggressive pitting environment (called Solution No. 20), including the addition of up to 4800 ppm peroxide to simulate radiolysis. This test, which was performed at 90°C for 2784 hours found a pitting corrosion rate of 9.17 $\mu\text{m}/\text{yr}$. Using the same assumptions for B and c as above, this results in an A of 6602 mm/yr . Based on this information it is considered conservative to use the value of A developed for exposure to 566°C superheated steam as a conservative representation of the corrosion behavior of Alloy 825 under continuously wetted conditions.

Conservative Approach to Pitting Corrosion (discounting waste package barriers)

Certain experimental and theoretical studies have concluded that Alloy 825 is subject to pitting corrosion which can rapidly penetrate the barrier in localized areas without having much metal weight loss overall so that the conventional experimental studies, summarized in the previous paragraph, fail to detect this potentially harmful process. For this reason the Sandia TSPA-93^(5.13) estimates a rapid corrosion process for Alloy 825 wherever it is contacted by a significant amount of water. For a Yucca Mountain repository environment, TSPA-93 predicts penetration of an Alloy 825 barrier in only a few hundred years. Since at least one study has found that Alloy 825 exhibits only broad shallow pits^(5.23), or none at all, in water of similar chemistry as that expected at the repository horizon, it may be concluded that further testing will either disprove the rapid pitting theory or will identify modified versions of Alloy 825 (such as high molybdenum) which are immune to rapid pitting. By the time of the next version of this document, we expect this issue may be resolved. In the meantime, as an alternative, we are presenting a conservative approach that has no barrier at all, since a corrosion time of a few hundred years is approximately zero on the time scale of tens of thousands of years considered here. These alternative, no-barrier, distributions will be further discussed in section 7.4.4.

Originator: J.R. Massari

Checker: J.K. McCoy

Pdf for Flood breach (f_2 for climate & tectonic)

Using the corrosion parameters identified above for carbon steel and Alloy 825, each of the six temperature histories shown in Figure 7.7 were evaluated using McCoy's model to predict waste package breach times for different locations in the repository. The time to penetrate the 120 mm thick dual-barrier waste package was determined by using the parameters for carbon steel until the penetration depth was equal to 100 mm (the thickness of the outer barrier), and then switching to the Alloy 825 parameters for the remaining 20 mm. Also, for the Alloy 825 barrier, c was taken to be 0.75 for the first 5000 years of inner barrier exposure, and 1.0 thereafter. This is equivalent to assuming the corrosion product layer becomes unprotective after 5000 years and leads to a conservative (lower) estimate of inner barrier lifetimes. The results of the evaluation are given in Table 7.2.

To determine the Weibull parameters for the waste package breach distribution, f_2 , the data produced by McCoy's model were plotted on Weibull probability paper. This plot is included as Attachment I. A value for θ was selected such that the plotted data formed a relatively straight line (a typical procedure for determining θ with this method). The value of β is then determined by drawing a line through the origin (\oplus) parallel to the plotted line. The value of α is determined by drawing a horizontal straight line at the 63.2% failure level until it intersects the plotted line, and then drawing a vertical line to the x-axis. The values of α , β , and θ obtained for the wetted waste package breach data in Table 7.2 were 280, 0.75, and 8000 respectively. The distribution of flooding waste package breach failures as a function of time, f_2 , is shown in Figure 7.8.

It should be noted that this analysis is independent of the density of corrosion pits per unit area of exposed metal. The assumption has been made that (1) if a single pit can penetrate the package surface, the package can be considered breached, and (2) the expected pit density is at least 1 per surface area of an individual package barrier.

Pdf for low infiltration breach (f_2 for wpb&ldl)

It is assumed that a fracture dripping at a low rate onto a waste package would be incapable of maintaining the surface of the package in a continuously wetted condition due to evaporation. This assumed intermittent wetting suggests that there will be a higher likelihood of starting corrosion pits at new locations, than continuing to extend their depth. Since there is no information on the corrosion behavior of the barrier materials under conditions of intermittent wetting it was assumed that the above behavior could be equally represented by general corrosion data from continuously immersed samples.

The most applicable data appears to be from a 9 week carbon steel corrosion test reported in the ASM Handbook^(5,20), which provided general corrosion rates for immersion in tuff groundwater at temperatures ranging from 50 to 100°C. These corrosion rates were found to be 0.4-0.5 mm/yr for the temperatures in the above range. Using an A of 1000 mm/yr,

Originator: J.R. Massari

Checker: J.K. McCoy

Stahl's value for B , and a c of 0.75, produces an average corrosion rate at 9 weeks time similar to that reported in the ASM Handbook. Therefore, these parameters will be used to represent the intermittent corrosion behavior of carbon steel in McCoy's model. *Since the intermittent wetting condition is assumed to be less aggressive than the continuously immersed condition*, the value for A (6602 mm/yr) developed in the wetting breach discussion from the study on pitting corrosion of Alloy 825 immersed in Solution No. 20 was used for the inner barrier. This environment is less aggressive than the superheated steam environment assumed for the wetting distribution, but should still represent a conservative estimate of degradation due to intermittent wetting. The Alloy 825 values for B and c remained the same as those used in the flooding breach discussion. The parameters for carbon steel and Alloy 825 were evaluated using McCoy's model and the blended temperature history from Figure 7.7, as described previously in the flooding breach discussion, to predict waste package breach times for different locations in the repository. The results of the evaluation are given in Table 7.4.

To construct f_2 from the results of the above analysis, the three parameter Weibull distribution was used as before to represent waste package breaches with time. As before, Weibull paper was used to determine the parameters for this distribution. Inspection of the data in Table 7.4 reveals that the packages nearest the center of the repository (12.5% range) breach later than those part-way out (50% range). It is evident that this is a direct result of the lower waste package surface temperatures predicted by Buscheck's model for the center-most group after the 10,000 year mark (see Figure 7.4). *As the center-most packages have the longest time to breach in the 50% range, the time to waste package breach reported for the 12.5% location was plotted at the 50% failure point on the Weibull plot; the time to breach at the 50% location was then plotted at the 37.5% failure point.* The remaining points were plotted according to their location on the temperature history as before. The Weibull paper yielded values for α , β , and θ of 5000, 1.75, and 30,000, respectively. The waste package breach failure distribution, f_2 , for a package located under a fracture dripping at a low rate, as described by these Weibull parameters, is shown in Figure 7.9.

Pdf for Corrosion breach at high infiltration (f_2 for wpb&ldh)

It is assumed that this flow rate would be sufficient to ensure that the surface of the waste package below the dripping fracture is continuously covered with a film of water. Therefore, the waste package breach distribution for high flow dripping, f_2 , will be taken to be the same as that developed for breach of the waste package in a flooded environment (Figure 7.8).

7.4.3.2 Corrosive leach of absorber/basket

To determine f_3 for the condition of a flooded environment, *it is first assumed that the boron and the surrounding stainless steel matrix will leach/dissolve together.* The fastest possible rate for this process was conservatively taken to be the same as the general

corrosion rate of Type 316 stainless steel immersed for 16 years in seawater at the Panama Canal, which was found to have experienced a corrosion rate of $1.25 \mu\text{m}/\text{yr}$ ^(5,16). Since the basket can be attacked on both sides this rate is doubled to get a minimum time to corrode 10 mm of Type 316 stainless steel of 4,000 years. The fraction of basket corrosion which can be tolerated depends on the actual SNF characteristics. The basket will have sufficient boron that 20% of the basket can be lost before any of the commercial fuel can exceed the 5% sub-critical safety margin with bias and uncertainty. *The conservative assumption has been made that a loss of 60% of the basket would permit no more than 50% of the expected fuel to exceed the safety margin.* A more precise analysis based the expected characteristics of the commercial fuel discharges is given in section 7.4.4 below, and shows this assumption to be very conservative. This 60%, or 6 mm thickness of basket material, would be removed in no less than 2,400 years of exposure to seawater. This time has been conservatively taken to be the lower limit (θ) of the Weibull distribution for f_3 .

Pdf for flood leach of absorber/basket (f_3 for climate & tectonic)

A literature search was performed to locate general corrosion data for Type 316 stainless steel in aqueous environments similar to that which might exist in a flooded drift. Information on the corrosion behavior of Type 304 stainless steels was also included because more extensive testing has been performed for Type 304 than 316, and because Types 304 and 316 were found to have relatively similar corrosion rates in tests which included both alloys. The corrosion rate information that was located is shown in Table 7.3, along with the estimated time at each rate to uniformly corrode 6 mm of material from both sides. The mean-time-to-corrode 6 mm of stainless steel in tuff groundwater, J-13 well water, and Solution No. 20 (bottom 7 rows in table) was found to be 19,823 years, with a standard deviation of 8,724 years (calculated using the @PUREAVG and @PURESTD functions in Lotus 1-2-3). Using this mean-time-to-failure (MTTF), standard deviation, and the value of θ determined in the preceding paragraph, the remaining parameters of the Weibull distribution were determined using the expressions,

$$MTTF = \theta + \alpha \Gamma(1 + 1/\beta) \quad (11)$$

and,

$$\sigma = \alpha \sqrt{\Gamma(1 + 2/\beta) - \Gamma^2(1 + 1/\beta)} \quad (12)$$

where $\Gamma(n)$ is the gamma function evaluated at n , using the Gamma Function Tabulation in the CRC Handbook^(5,18). The parameters α and β were found to be 19,675 and 2.1, respectively. The resulting distribution, f_3 , is shown in Figure 7.10.

Although the deterministic component of general corrosion is evident, the following aspects of the random component of the process should be noted in justification of the use of a probability distribution:

1. Wide distribution of corrosion rates in the literature, even for seemingly similar water chemistry.
2. Experimental observations typically show corrosion rates which decrease with time on any given sample due to passivation. Random convective mixing within the filled package may remove this passive layer from some areas, leaving fresh surface for more rapid corrosion.
3. Temperature variations from one package to another will lead to different convection rates, which cause variations in corrosion rates according to the previous item. Package to package variations in convection rate will also cause variations in boron concentration remaining near the leaching basket material, where it can still be an effective, criticality suppressing, neutron absorber.
4. There will be local differences in water chemistry from one waste package interior to another, due to differences in travel paths through the partly corroded containers.
5. There are many tests in freshwater (lake and river) which show no measurable corrosion of Type 316 stainless steel for exposure times up to 16 years, suggesting that there is a significant tail on the high side of the distribution.
6. In order to permit criticality, the leached boron must be removed from the interior volume of the waste package, either by water flow out large holes, or by plating on the inner package walls as the water seeps through some slowly flowing leak. Both of these are random processes.

Pdf for low infiltration leach of absorber/basket (f_3 for wpb&ldl)

The neutron absorber leach rate distribution, f_3 , was developed by modification of the lower limit, mean-time-to-corrode, and standard deviation developed for 6 mm of stainless steel under flooded condition. As before, this modification was based on the results of general corrosion test data for Types 304 and 316 stainless steel, and a further search of the available literature was performed to locate corrosion tests of intermittently wetted samples. *This test condition was felt to be more applicable to overhead dripping than that of the continuous immersion tests used for flooding, because the level of water in the basket of a breached WP may change with time due to fluctuations in the drip rate, evaporation rate, or the formation of drainage holes.* One study of Type 316 stainless steel placed at the mean tide level of the Panama Canal (seawater) for 16 years was found to have experienced a corrosion rate of $0.16 \mu\text{m}/\text{yr}^{(5,16)}$. Another test that was performed for 304L stainless steel in aerated simulated J-13 well water at 90°C for 1.5 years

Originator: J.R. Massari

Checker: J.K. McCoy

determined general corrosion rate to be $<0.005\mu\text{m}/\text{yr}$ through measurements of weight loss^(5.23). In this test, the solution was allowed to evaporate, and new solution was added on a weekly basis. Comparison of the above test results with the immersion data in Table 7.3 reveals that the intermittently wetted corrosion rates may be an order of magnitude lower than those for complete immersion under the same conditions. *Therefore, it is felt that doubling of the flooding leach lower limit, MTTF, and standard deviation should result in a conservative distribution of the time to corrode 6 mm of material (thus leaching 60% of the boron).* Doubling of the above mentioned parameters results in a θ of 4800 years, a MTTF of 39,646 years, and a standard deviation of 17,448. Using the Weibull expressions for MTTF and standard deviation presented in the flooding breach and leach discussion, α and β were determined to have values of 39350 and 2.1, respectively. The resulting distribution, f_3 , is shown in Figure 7.11.

Pdf for high infiltration leach of absorber/basket

The neutron absorber leach distribution, f_3 , will be that used for the low flow rate dripping described above (Figure 7.11).

Originator: J.R. Massari

Checker: J.K. McCoy

7.4.4 Probability of sufficient fissile material in a package

After all the hazard events that are necessary for a criticality event (WP breach, absorber leach, and internal flooding) have occurred, there is still one fundamental requirement for each scenario: the SNF must have the right combination of high enough fissile material and low enough burnup to become critical. The criticality capability is determined by k_{eff} . Deterministic neutronics calculations of k_{eff} for a range of values for age, for specific burnup and initial enrichment indicate that after emplacement, most assemblies will have a peak in criticality potential at approximately 10,000 years. In particular, 21 PWR assemblies having 3% initial enrichment and 20 GWd/MTU burnup (waste package criticality design basis fuel) in a waste package design with stainless steel basket, will have a peak $k_{\text{eff}}=0.965$ at 10,000 years which is followed by a slow decline to $k_{\text{eff}}=0.932$ at 200,000 years (Ref. 5.7, Figure 6.8.3-5). The physical requirement to avoid criticality is $k_{\text{eff}} < 1.0$. For licensing calculations it is usually required that $k_{\text{eff}} \leq 0.95$, which provides a 5% safety factor. In addition, there is usually an additional amount (typically up to 0.06) to be subtracted for bias and error. For this analysis the dividing line for determining criticality is $k_{\text{eff}}=0.95$. This provides a conservative probabilistic estimate of what will actually happen, but not, necessarily conservative enough to license a waste package with respect to a deterministic estimate of worst case performance.

To determine the fraction of the packages which will have $k_{\text{eff}} \geq 0.95$, we use the Design Basis Fuel Analysis^(5.25) which tabulated SNF statistics with respect to k_{∞} using a parameterization of k_{∞} developed by ORNL^(5.26) for PWR fuel using 210 SCALE runs that covered a representative range of values of age, burnup, and initial enrichment. In this tabulation an age of 5 yrs was used. The correspondence between k_{∞} and k_{eff} is then determined by calculating k_{∞} from the formula given by ORNL^(5.26) for the design basis fuel (age=5 yrs, burnup=20 GWd/MTU, initial enrichment=3%), with the result $k_{\infty}=1.138$. An MCNP calculation showed this criticality design basis fuel to have a k_{eff} approximately equal to 0.98, so the difference between k_{∞} and k_{eff} is 0.158. We now interpret Ref. 5.7, Figure 6.8.3-5, as follows: (1) for times of interest (2,000 to 200,000 years) determine the difference between 0.95 and k_{eff} , (2) add that difference to 1.138 to determine the k_{∞} which would correspond to a $k_{\text{eff}}=0.95$, (3) consult the tabulation of k_{∞} percentiles in Ref. 5.25 to determine the percentage of SNF which would have a higher k_{∞} . The results are given in Figure 7.12. This factor will be used as a multiplier on each of the three conditional breach and leach pdf's produced in section 7.4.5, to determine the corresponding breached, leached, and capable of criticality cdf.

An external criticality event would be expected to require a longer time (more waste package barrier corrosion, and extensive breaching of the fuel element cladding) than the internal criticality event sequences discussed thus far. Hence the probability of occurrence is correspondingly smaller, and has not been extensively studied thus far. Nevertheless, since this is an important topic, the final draft of this document will contain an estimate of the probability of the fuel being reconfigured into a flat plate mixture with moderator (water), and the k_{eff} which could result.

Originator: J.R. Massari	Checker: J.K. McCoy
--------------------------	---------------------

7.4.5 Evaluations of two-fold convolutions of pdf's

The pdf for the combined flow, breach and leach events was obtained from the convolution of f_1 , f_2 and f_3 . This convolution was computed by a Monte-Carlo numerical integration which used a Lotus 1-2-3 spreadsheet to randomly sample the cdf for each distribution and sum the times to reach the defined flow (or flood) condition, to breach the waste package and to leach 60% of the boron. Eight thousand trials were performed. Probabilities of occurrence for each of the three conditional breach and leach event sequences at 20,000 years after emplacement, and 40,000 through 200,000 years in 40,000 year intervals, are summarized in Table 7.5. Each of the three individual event sequences is further discussed below. The Lotus 1-2-3 Monte Carlo convolution method was independently verified using an alternate method of calculation, as described in Attachment III.

As discussed previously, due to apparently conflicting theories on the pitting corrosion behavior of Alloy 825, it was also decided to investigate a worst-case scenario in which the waste package barriers were penetrated in a relatively short period of time compared to the other events in the sequence. This was performed for each of the three event sequences by simply eliminating f_2 from the convolution, effectively producing conditional breach and leach distributions which consider the barrier to be instantly breached upon the occurrence of the initiating event. The convolutions were performed using the Lotus 1-2-3 spreadsheet in the same manner as above.

Flooding Convolution (climate & tectonic)

The probability distribution resulting from the convolution of the flooding, breach, and leach distributions is summarized in Figure 7.13. The cdf, which is also shown in Figure 7.13 is then computed by numerically integrating the pdf multiplied by the time dependent critical fuel fraction developed in 7.4.4. The fluctuations in the pdf are due to the random nature of the Monte-Carlo process. Detailed examination of the convolution reveals that the first occurrence of all three events in the sequence (hereafter referred to simply as "failure") happens at approximately 50,000 years after emplacement, with the last failure occurring at 10,050,000 years. Thus, the conditional probability of failure due to flooding prior to 50,000 years is essentially zero. The conditional probabilities of flooding breach and leach at 20,000, 40,000, 80,000, 120,000, 160,000, and 200,000 years after emplacement, as determined from the cdf, have been summarized in Table 7.5. Due to the low number of flooding events occurring in this time frame, the Monte-Carlo generated cdf was recalculated 20 times, and the results from each calculation were averaged, for each of the above times, to obtain better statistical estimates of the conditional probabilities. The conditional probabilities for later times may be obtained by inspection of the cdf in Figure 7.13. The probabilities developed for the no-barrier convolution are also summarized in Table 7.5. The no-barrier distribution is not shown due to the fact that it is visually indistinguishable from Figure 7.13.

Originator: J.R. Massari	Checker: J.K. McCoy
---------------------------------	----------------------------

Low Infiltration Convolution (wpb&ldl)

The probability distribution and cdf resulting from the convolution of the low infiltration, breach, and leach distributions is summarized in Figure 7.14. Detailed examination of the convolution reveals that the first failure happens at approximately 38,500 years after emplacement, with the last failure occurring at 166,250 years. Thus, the conditional probability of failure due to high infiltration prior to 38,500 years is essentially zero. The conditional probabilities of low infiltration breach and leach, as determined from the cdf, have been summarized in Table 7.5. The conditional probabilities for other times may be obtained by inspection of the cdf in Figure 7.14. The probabilities developed for the no-barrier convolution are also summarized in Table 7.5. The no-barrier distribution is shown in Figure 7.16. The first failure in the alternate low infiltration sequence occurs at 7,750 years.

High Infiltration Convolution (wpb&ldh)

The probability distribution and cdf resulting from the convolution of the high infiltration, breach, and leach distributions is summarized in Figure 7.15. Detailed examination of the convolution reveals that the first failure happens at approximately 18,500 years after emplacement, with the last failure occurring at 200,500 years. Thus, the conditional probability of failure due to high infiltration prior to 38,500 years is essentially zero. The conditional probabilities of high infiltration breach and leach, as determined from the cdf, have been summarized in Table 7.5. The conditional probabilities for other times may be obtained by inspection of the cdf in Figure 7.15. The probabilities developed for the no-barrier convolution are also summarized in Table 7.5. The no-barrier distribution is shown in Figure 7.17. The first failure in the alternate high infiltration sequence occurs at 8,500 years.

Originator: J.R. Massari**Checker: J.K. McCoy**

7.4.6 Probability of sufficient moderator (corrosion hole configuration favorable to ponding of dripping water in waste package)

For the overhead dripping scenarios, there must be holes around the middle of the package, but not the lower part. The most likely location is on the upper surface which is most exposed to dripping water. *The conditional probability of such a hole configuration, given that there is sufficient corrosion to produce the holes in the first place, is the product of the conditional probability of holes around the middle (0.1) and the conditional probability of no holes in the lower half, given that there are holes around the middle (0.1).* This latter probability is actually quite conservative, since half of the weld around the lid will be in the lower, submerged, half of the horizontal package, and this weld is more likely to corrode and leave a hole to prevent ponding. On the other hand, there is a possibility that the leached/corroded material could plug up such holes, so that subsequent ponding could be supported even if the initial hole configuration were not favorable to ponding. This analysis will be refined in the next few years; by the time of license application it will include:

- More precise modeling of corrosion from dripping, particularly in welds.
- Fluid dynamic modeling of leach and ponding processes, including the effects of alternative hole configurations.
- Deterministic evaluation of criticality for likely flooding and assembly geometry configurations.

7.4.7 Probability that Fuel Assemblies Maintain Geometry Required For Criticality (geometry)

Since criticality of SNF assemblies will require nearly full moderation, there can be no criticality if the basket and assembly hardware fail in such a way that the fuel rods can collapse into a consolidated configuration which does not permit sufficient water between the rods. Such a collapse would generally require the corrosion of the fuel cladding or grid spacers in each assembly. *It is conservatively assumed that the fuel assemblies will always maintain a geometry which supports optimal moderation for the time frame covered by the current analysis.* Therefore, this event has a probability of 1.0. This analysis will be refined in the next few years; by the time of license application it will include:

- More precise modeling of the fuel assembly structural failure distribution following loss of the inert environment;
- Deterministic evaluation of the criticality potential of other possible geometries which could be formed prior to complete degradation of the waste package structure.

Originator: J.R. Massari

Checker: J.K. McCoy

Table 7.2. Immersed WP Time To Breach Predicted By McCoy's Model

Repository Location	Time To Breach (Years Since Emplacement)	
	Outer Barrier Breached	Inner Barrier Breached
12.5%	680.9	8056
50%	681.1	8117
75%	688.4	8452
90%	762.0	9181
97%	876.6	9781
99%	923.9	9886

Note: These predicted barrier lifetimes are specifically for the scenario of a drift that floods and remains flooded as soon as WP surface temperatures fall below 100°C.

Table 7.3. General Corrosion Data For Types 304 & 316 Stainless Steel

Stainless Steel Type	Test Environment	Test Temp (C)	Test Duration (years)	Corrosion Rate (µm/yr)	Time To Corrode 6mm (y)	Ref.
316	Seawater Immersion	≈27	16	1.25	2,400	5.16
316	Seawater Immersion	≈27	1	14.99	200	5.16
316	Seawater Mean Tide	≈27	16	0.16	18,750	5.16
316L	J-13 Immersion	50	1.3	0.154	19,481	5.21
304L	J-13 Immersion	50	1.3	0.133	22,556	5.21
304L	J-13 & 6E5 rads/hr	28	1	0.0811	36,991	5.21
304L wld	J-13 & 6E5 rads/hr	28	1	0.123	24,390	5.21
304L	J-13 Immersion	90	0.22	0.29	10,344	5.17
304L	Sol. 20 Immersion	90	0.33	0.2	15,000	5.17
304L	Tuff Groundwater at 3E5 & 6E5 rads/hr	?	0.15	0.3	10,000	5.20

Originator: J.R. Massari

Checker: J.K. McCoy

Table 7.4. Time To Breach WP Under Low Rate Drip Predicted By McCoy's Model

Repository Location	Time To Breach (Years Since Emplacement)	
	Outer Barrier Breached	Inner Barrier Breached
12.5%	3150.1	34807.3
50%	3198.2	33364.5
75%	3496.4	34850
90%	4402.6	38286.2
97%	5279.5	40843.4
99%	5579.7	41665.6

Note: These predicted barrier lifetimes are specifically for the scenario of a WP located below a fracture that begins continuously dripping at a low rate as soon as WP surface temperatures fall below 100°C.

Originator: J.R. Massari**Checker:** J.K. McCoy

Table 7.5. Summary of Fault Tree Event Probabilities For Various Times Since Emplacement

Time Emplaced (years)	Basic and Conditional Event Probabilities					
	holes	crackswp	geometry	climate & tectonc	wpb&ldl	wpb&ldh
<i>WP Barriers Provide Temporary Protection Against Moderator Entry</i>						
20,000	1.00x10 ⁻²	8.54x10 ⁻²	1.00	0	0	6.70x10 ⁻⁶
40,000	1.00x10 ⁻²	8.54x10 ⁻²	1.00	0	6.21x10 ⁻⁶	1.57x10 ⁻³
80,000	1.00x10 ⁻²	8.54x10 ⁻²	1.00	1.97x10 ⁻⁶	2.41x10 ⁻²	1.44x10 ⁻²
120,000	1.00x10 ⁻²	8.54x10 ⁻²	1.00	4.75x10 ⁻⁶	4.27x10 ⁻²	3.12x10 ⁻²
160,000	1.00x10 ⁻²	8.54x10 ⁻²	1.00	8.09x10 ⁻⁶	4.36x10 ⁻²	4.10x10 ⁻²
200,000	1.00x10 ⁻²	8.54x10 ⁻²	1.00	1.29x10 ⁻⁵	4.36x10 ⁻²	4.21x10 ⁻²
<i>WP Barriers Given No Credit For Preventing Moderator Entry</i>						
20,000	1.00x10 ⁻²	8.54x10 ⁻²	1.00	0	2.87x10 ⁻³	1.75x10 ⁻⁴
40,000	1.00x10 ⁻²	8.54x10 ⁻²	1.00	3.36x10 ⁻⁷	2.14x10 ⁻²	3.26x10 ⁻³
80,000	1.00x10 ⁻²	8.54x10 ⁻²	1.00	2.84x10 ⁻⁶	4.67x10 ⁻²	1.87x10 ⁻²
120,000	1.00x10 ⁻²	8.54x10 ⁻²	1.00	5.50x10 ⁻⁶	4.86x10 ⁻²	3.54x10 ⁻²
160,000	1.00x10 ⁻²	8.54x10 ⁻²	1.00	1.05x10 ⁻⁵	4.86x10 ⁻²	4.24x10 ⁻²
200,000	1.00x10 ⁻²	8.54x10 ⁻²	1.00	1.71x10 ⁻⁵	4.86x10 ⁻²	4.30x10 ⁻²

Originator: J.R. Massari	Checker: J.K. McCoy
---------------------------------	----------------------------

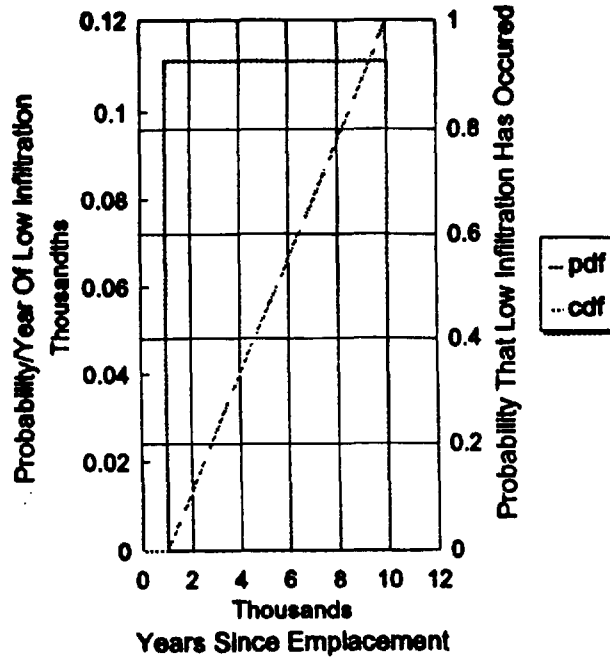


Figure 7.4. Distribution of time-to-occurrence of the low infiltration initiating event.

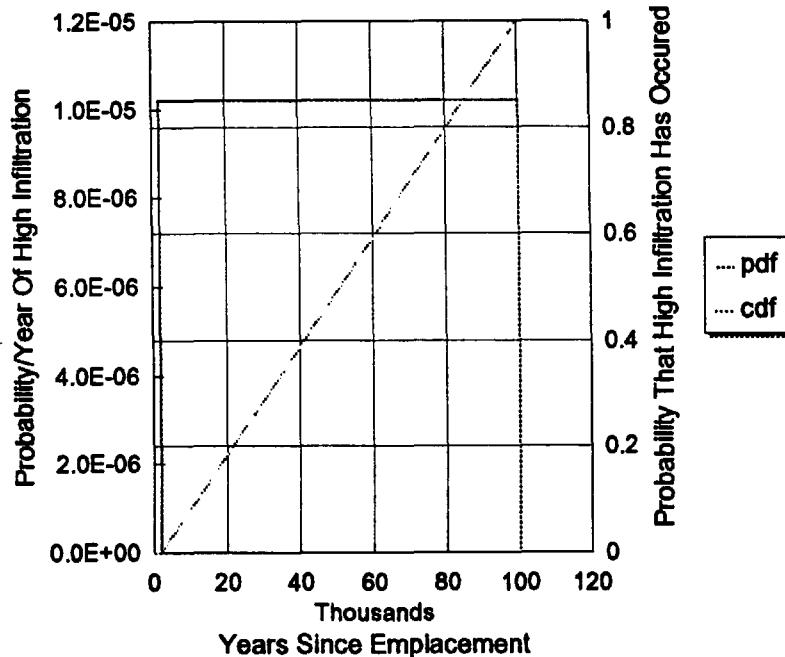


Figure 7.5. Distribution of time-to-occurrence of the high infiltration initiating event.

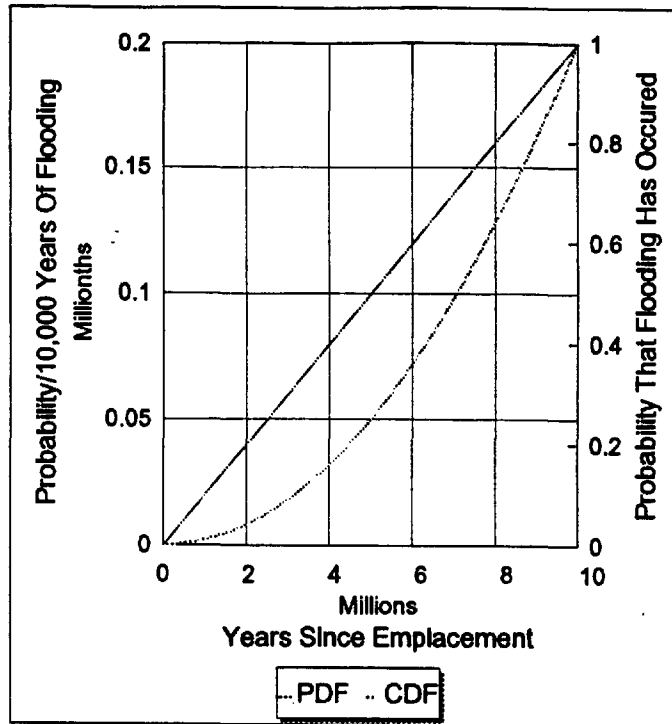


Figure 7.6. Distribution of time-to-occurrence of repository flooding

Originator: J.R. Massari

Checker: J.K. McCoy

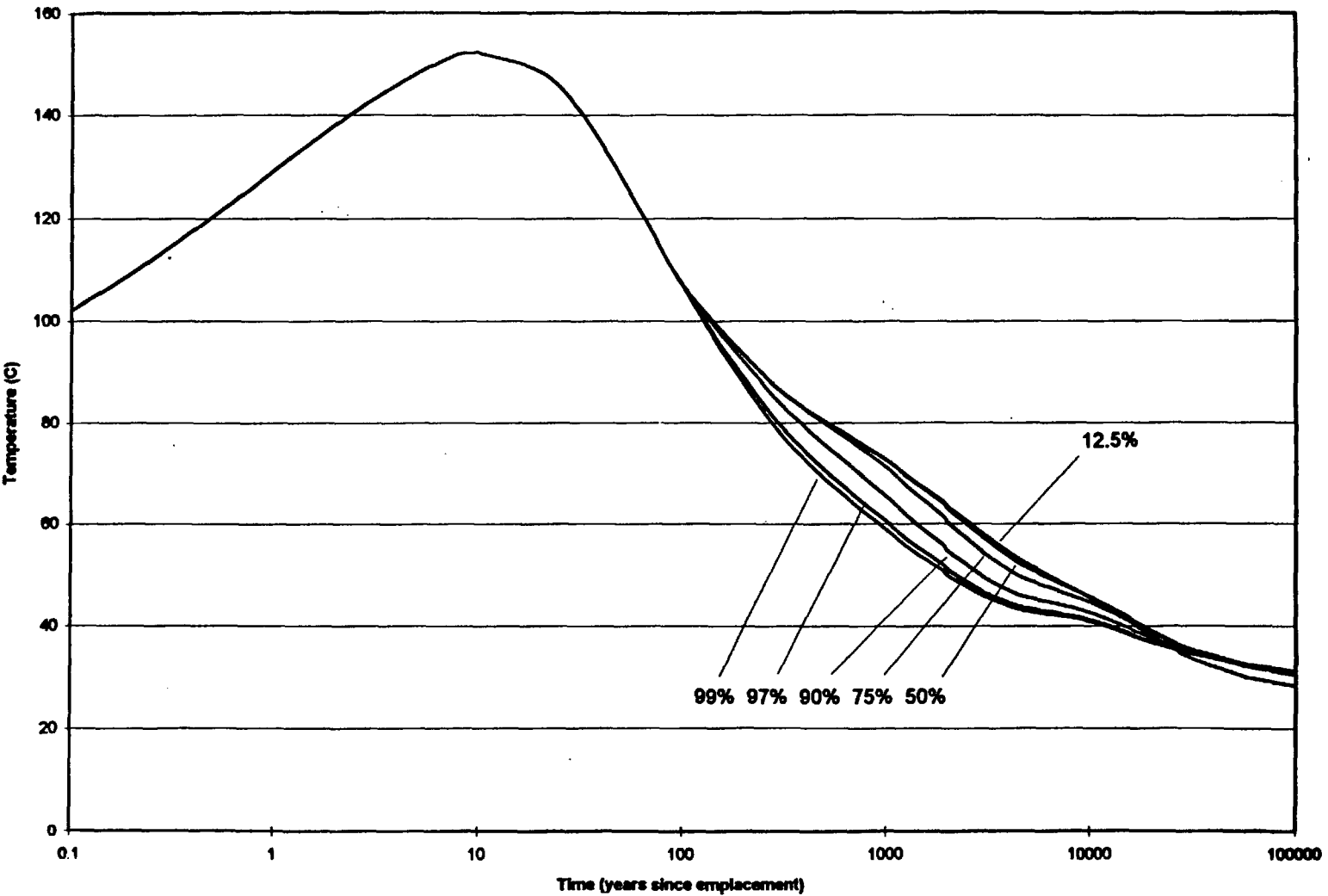


Figure 7.7. Waste Package surface temperature as a function of time for a mass loading of 6.0 kg U/m² (approximately 24 MTU/acre), curves are for different locations in the repository (0% - center, 25% - mid-way from center to edge, 100% - edge)

Originator: J.R. Massari

Checker: J.K. McCoy

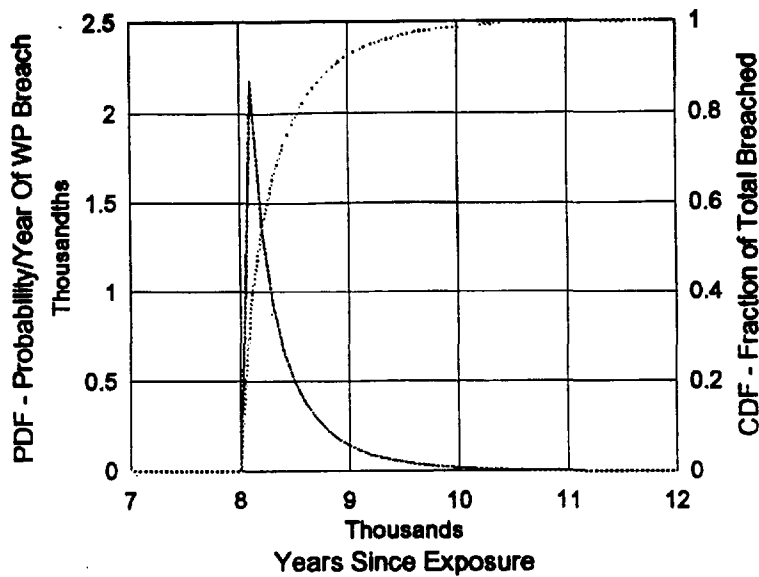


Figure 7.8. Distribution of WP breach failures developed using McCoy's model and assuming that drift floods and remains flooded as soon as WP surface temperature falls below 100°C

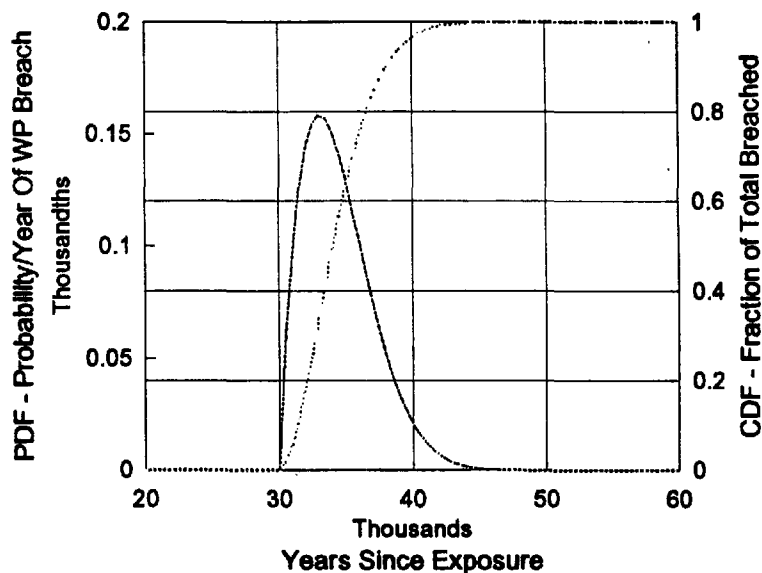


Figure 7.9. Distribution of WP breach failures developed using McCoy's model and assuming that WP located under fracture continuously dripping at a low rate

Originator: J.R. Massari	Checker: J.K. McCoy
--------------------------	---------------------

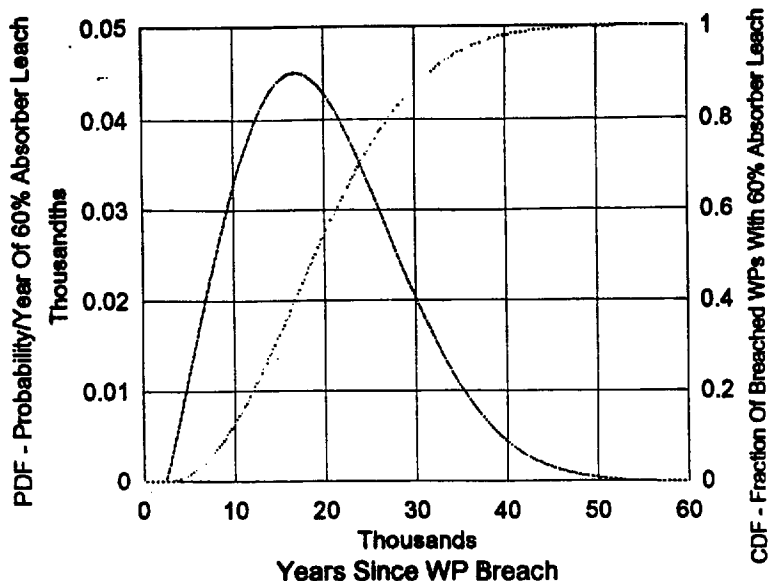


Figure 7.10. Distribution of time to leach 60% of neutron absorbing material from UCF-WP basket structure assuming WP remains continuously immersed in flood waters

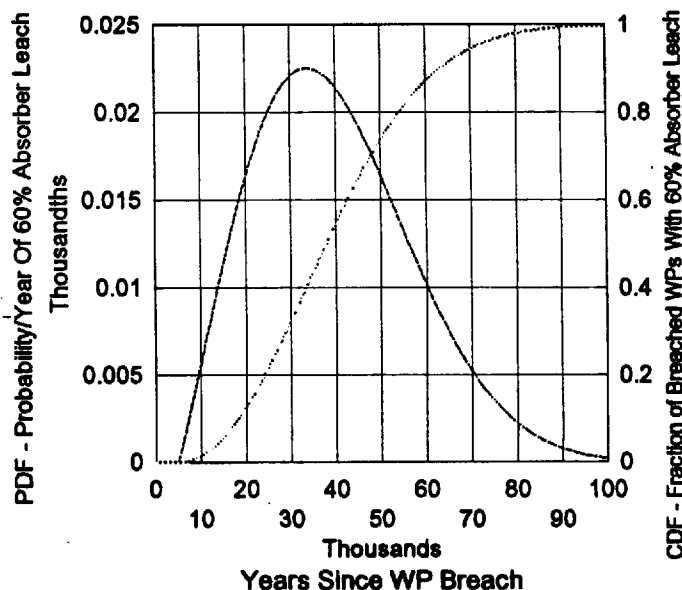


Figure 7.11. Distribution of time to leach 60% of neutron absorbing material from UCF-WP basket structure assuming WP is exposed to a continuously dripping overhead fracture

Originator: J.R. Massari	Checker: J.K. McCoy
--------------------------	---------------------

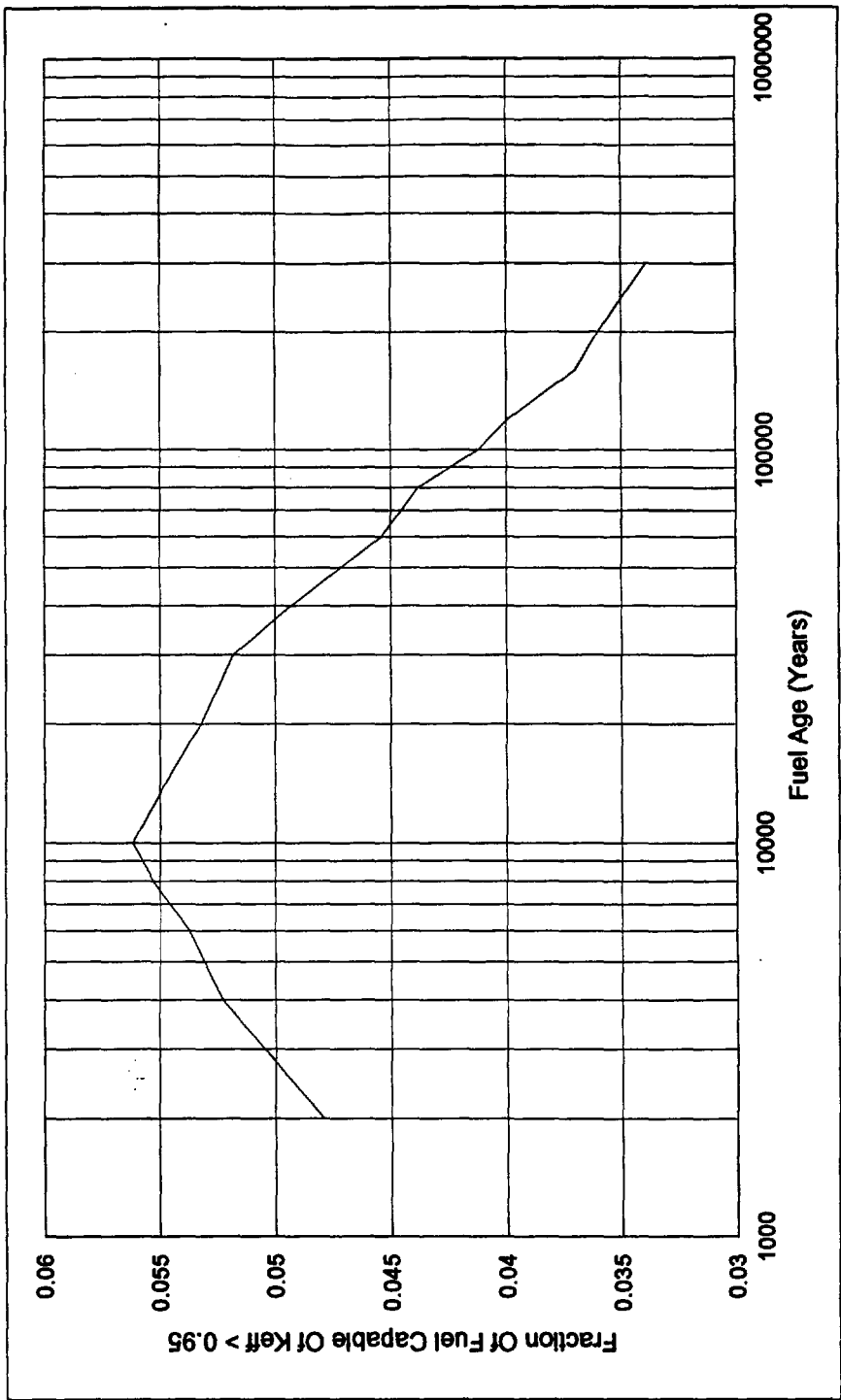


Figure 7.12. Fraction of design basis fuel (3% initial enrichment, 20 GWd/MTU Burnup) as a function of time capable of achieving $k_{eff} > 0.95$ in an UCF-WP geometry with no neutron absorber in the basket structure

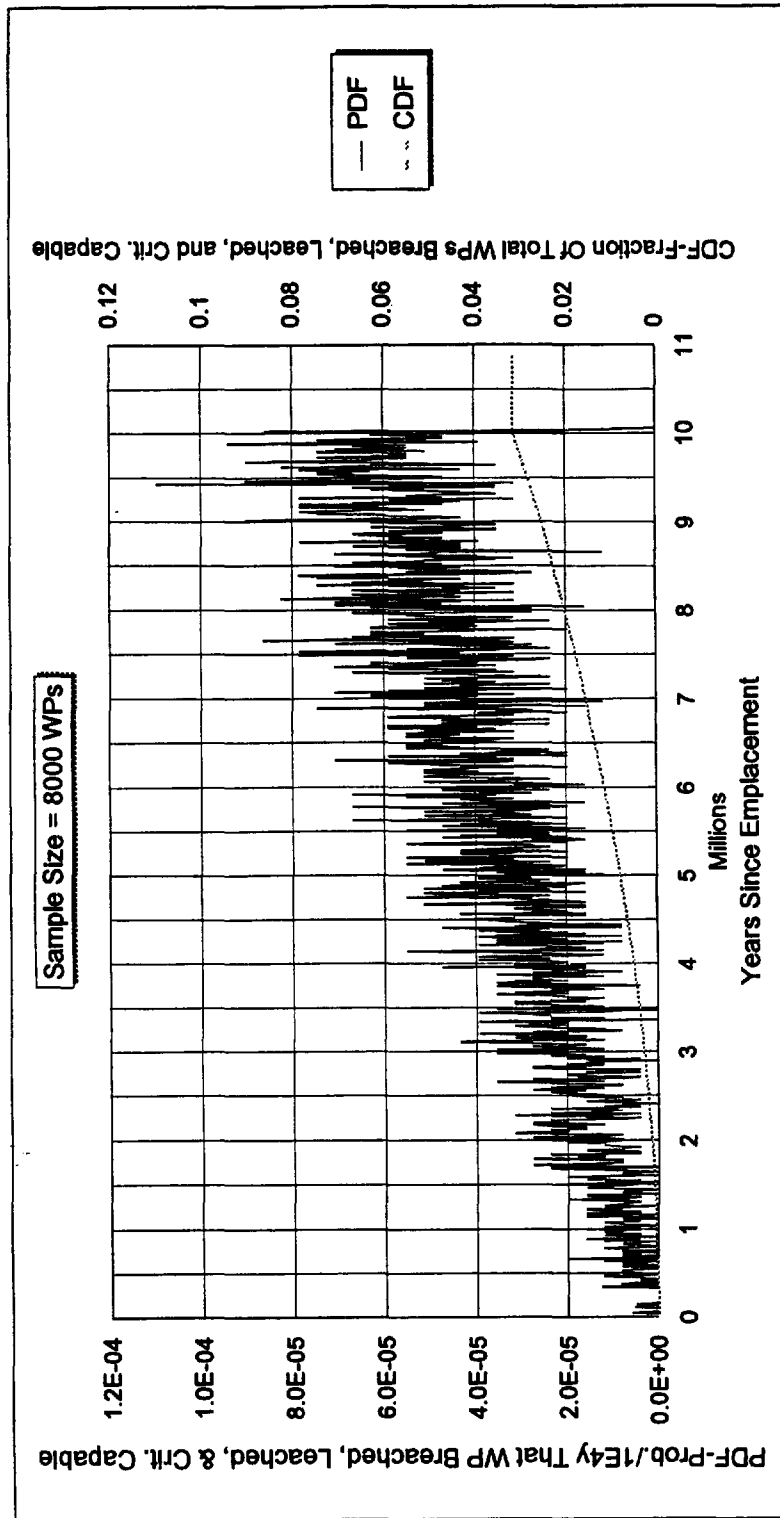


Figure 7.13. Convolution of the three distributions for repository flooding occurrence, UCF-WP breach given flooding and 60% boron leach given flooding

Originator: J.R. Massari

Checker: J.K. McCoy

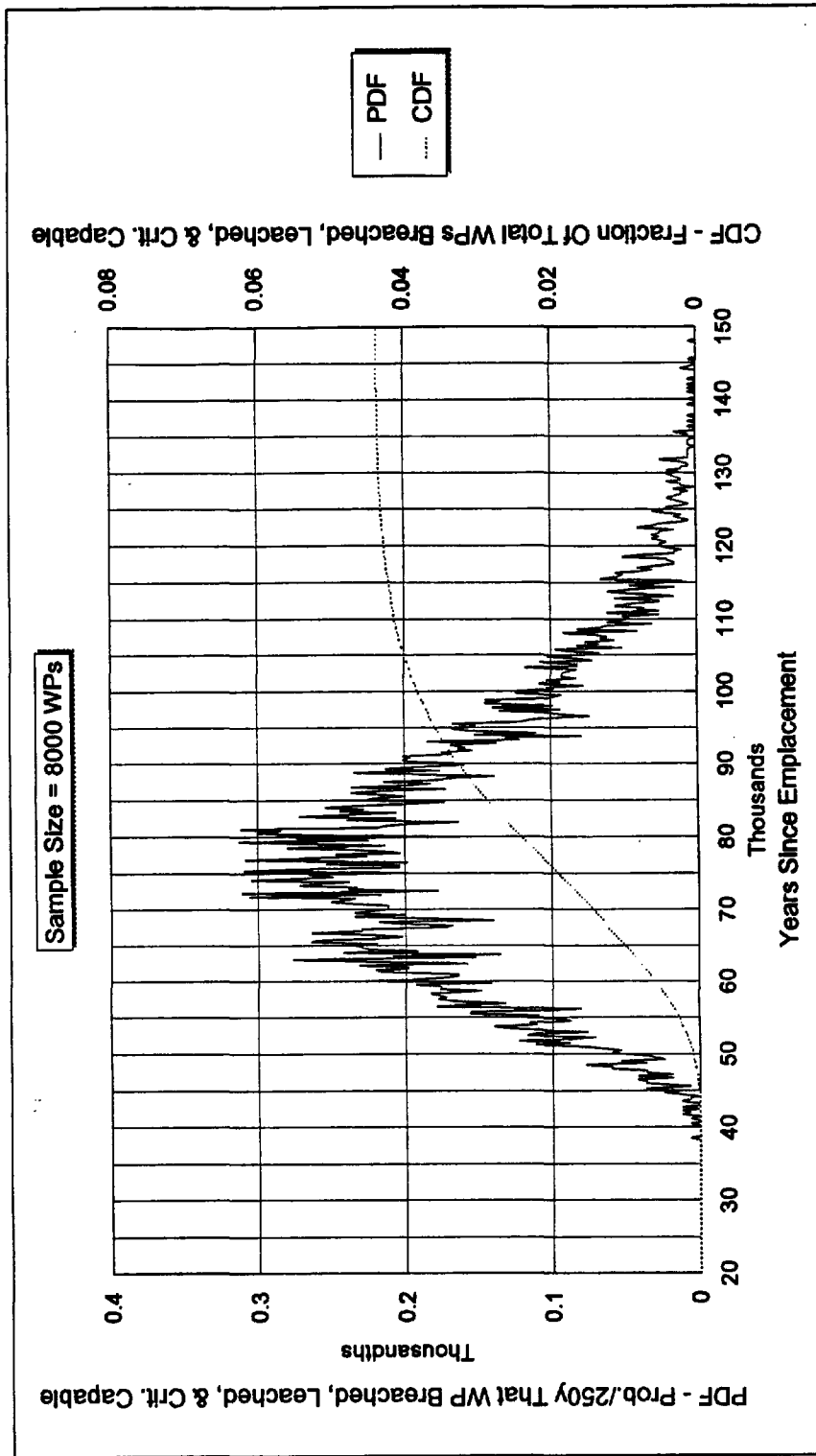


Figure 7.14. Convolution of three distributions for low infiltration occurrence, WP breach given low-rate dripping, and 60% boron leach given low-rate dripping

Originator: J.R. Massari

Checker: J.K. McCoy

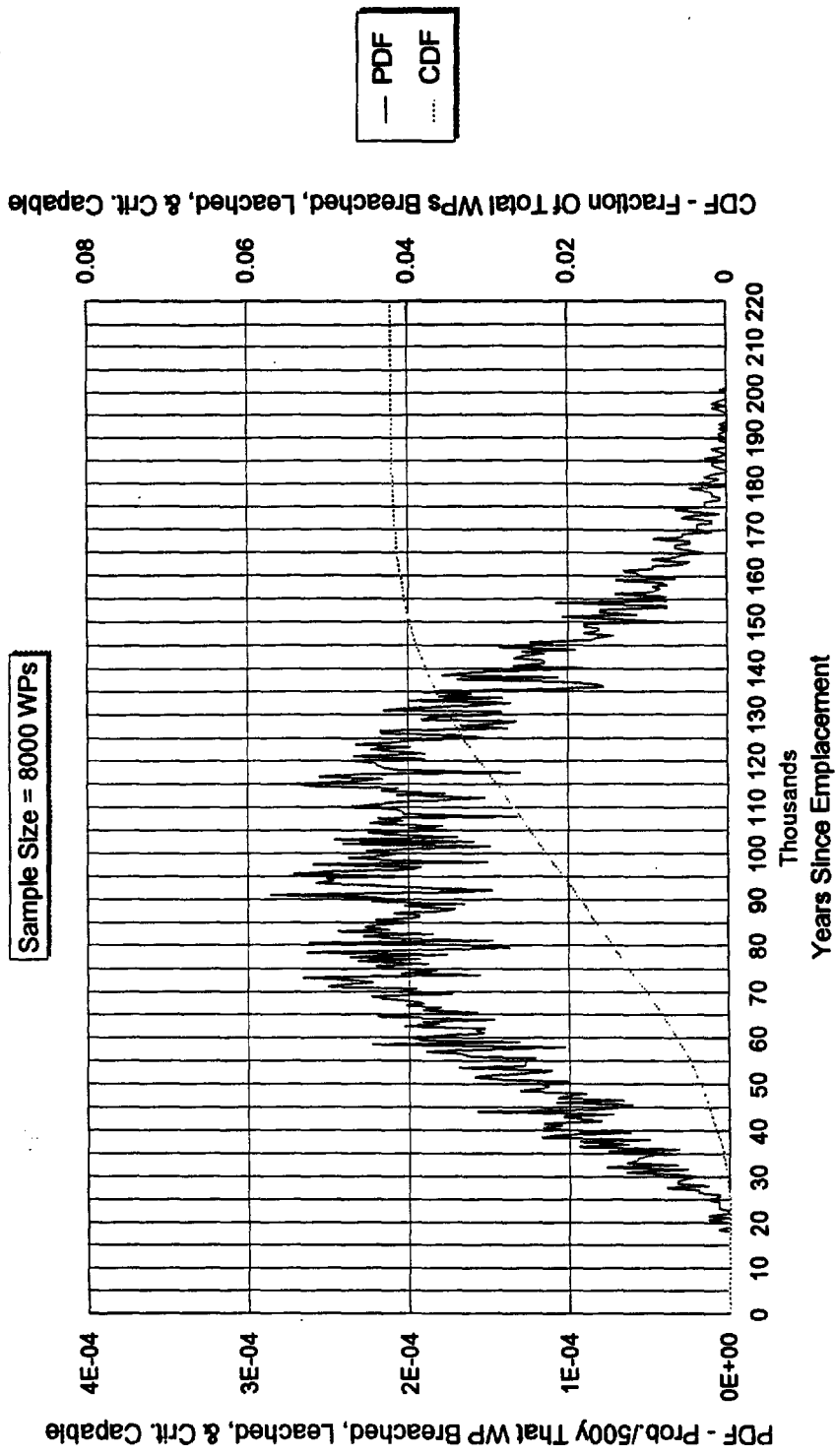


Figure 7.15. Convolution of tree distributions for high infiltration occurrence, WP breach given high-rate dripping, and 60% boron leach given high-rate dripping

Originator: J.R. Massari	Checker: J.K. McCoy
--------------------------	---------------------

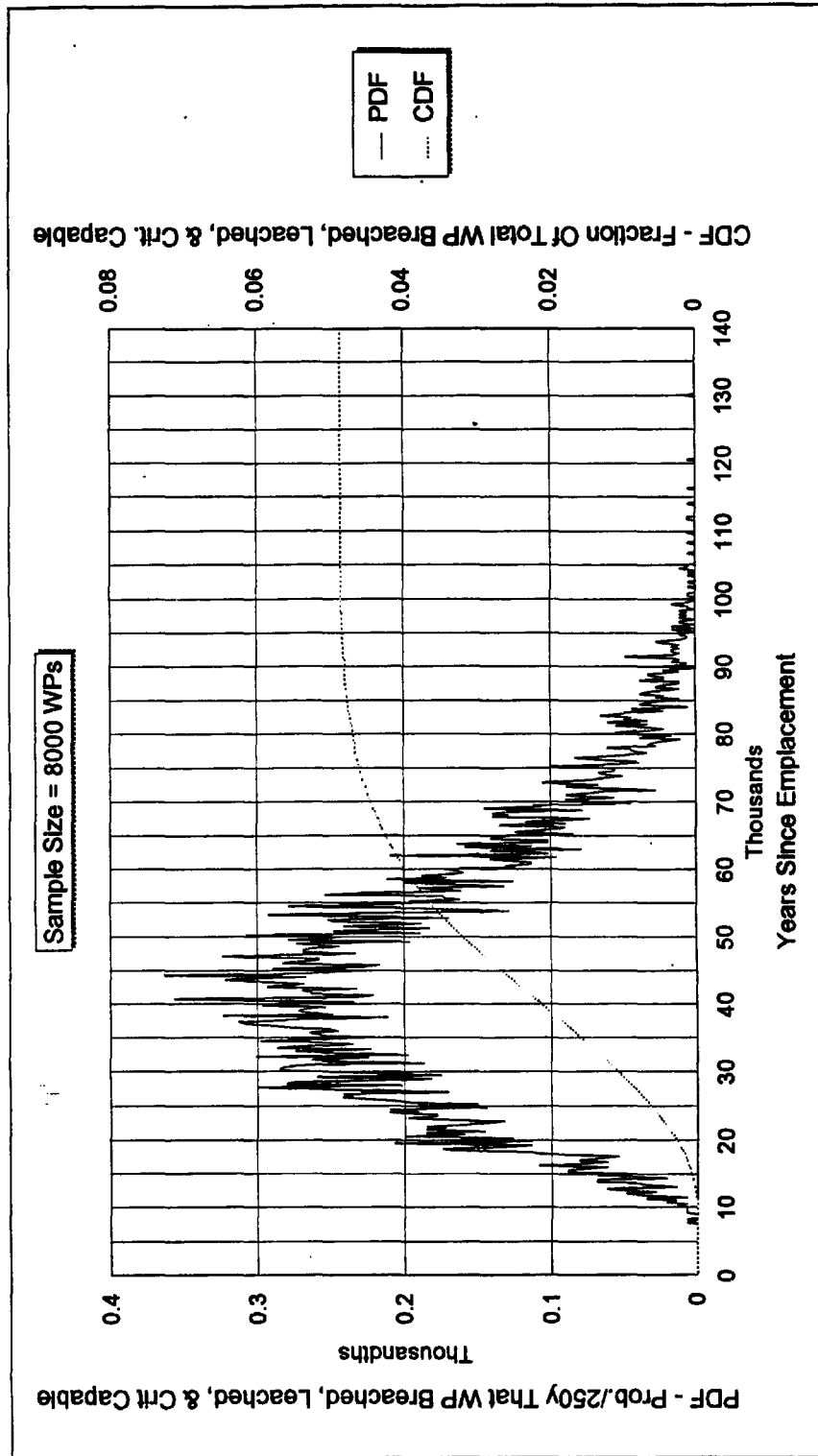


Figure 7.16. Alternate "no-barrier" convolution of the two distributions for low infiltration occurrence, and 60% boron leach given low-rate dripping

Originator: J.R. Massari

Checker: J.K. McCoy

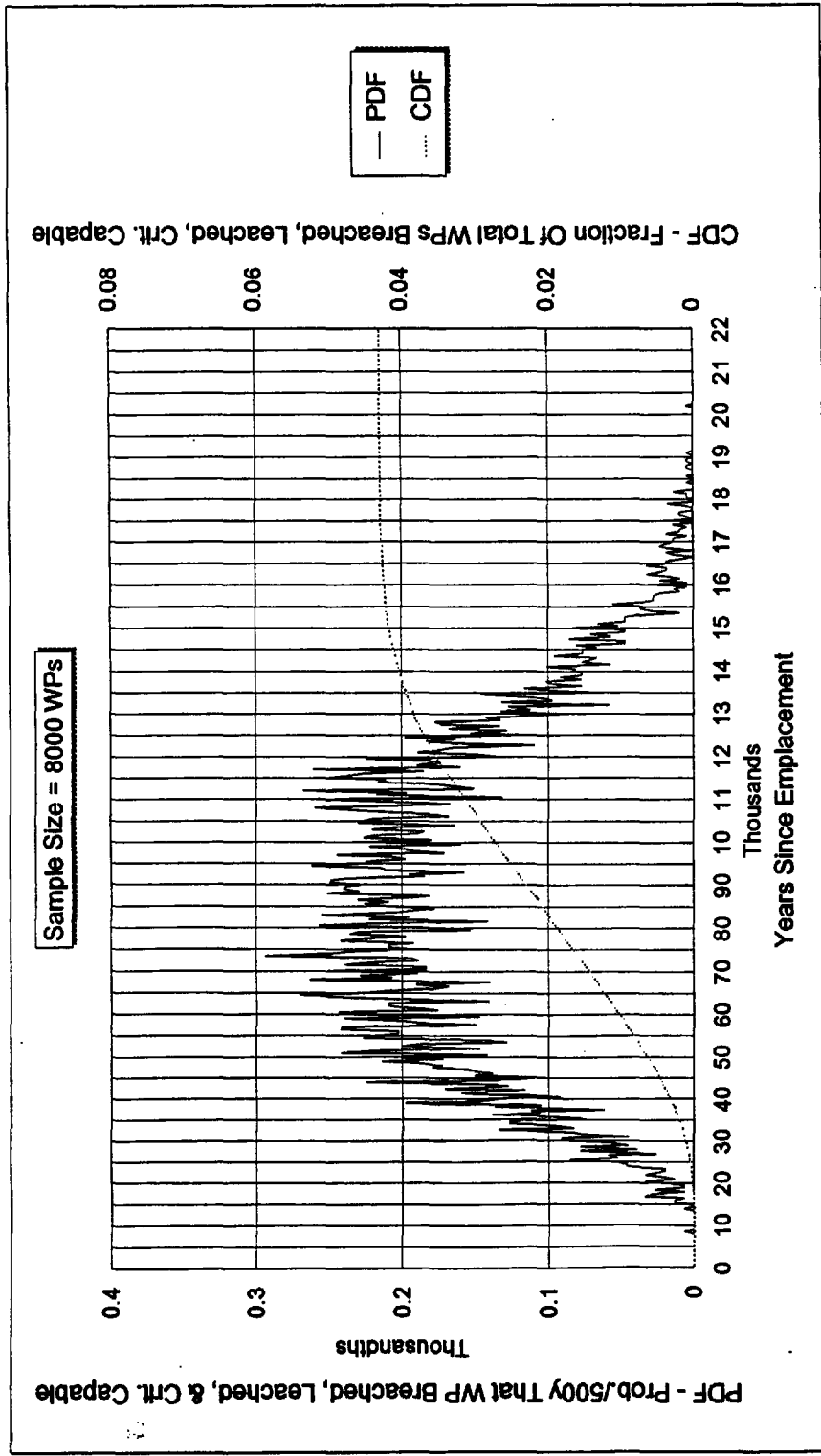


Figure 7.17. Alternate "no-barrier" convolution of the two distributions for high infiltration occurrence, and 60% boron leach given high-rate dripping

7.5 Fault Tree Analysis

In this section, the basic and time dependent conditional event probabilities developed in Section 7.4 are input into the fault tree developed in Section 7.3. The fault tree was evaluated at the times after emplacement for which conditional event probabilities were quoted in Table 7.5. Since all basic event probabilities are on a per package basis, and all conditional probabilities are dimensionless, the fault tree top event will also be in terms of a criticality probability per package at a given point in time. This differs from the typical top event units for a fault tree of an active system of components, (such as a nuclear power plant safety system) which is usually expressed as a system failure rate or a probability of system failure in a given mission time. This is appropriate when the failure rates of the system components can be treated as constants and the mission time is relatively short when compared to the mean-time-to-failure of the components. However, when the majority of events are conditional on other events and have time dependent failure rates, as is the case in the current analysis, the top event is more useful as a pointwise probability (cdf evaluated at specific points in time). Evaluating the fault tree at various times will then produce a cumulative distribution for the occurrence of the top event (i.e., waste package criticality).

The fault tree top event was quantified using CAFTA version 2.3 fault tree analysis software. This software first determines the various sequences of events, or "cutsets", which can lead to the occurrence of the top event, and determines their probabilities. The probability of a given cutset is simply the product of the probabilities of all events in the cutset sequence. (Recall that the probabilities of the most significant events are actually cdf's determined from two-fold convolutions described in 7.4.4.) As evaluation of the fault tree was performed from CAFTA's Fault Tree Editor module using the Evaluate command, CAFTA used the default bottom-up approach of successive substitution to determine the minimal cutsets for the fault tree. The top event probability is then calculated using the min-cut-upper-bound calculation

$$P(\text{TopEvent}) = 1 - \prod_{i=1}^n [1 - P(C_i)]$$

where $P(C_i)$ is the probability of the i^{th} cutset and n is the total number of cutsets. This calculation is better than a simple sum as it will never be higher than 1.0, but will give a conservative upper limit.

Results of the quantification of the fault tree top event at each of the previously selected timesteps is given in Table 7.5. The individual cutsets which make up the top event probability, and their contribution to the top event is also shown. A visual representation of the quantified fault tree at the 80,000 year timestep is provided in Figure 7.18. Table 7.6 provides the results of the quantifications performed for the alternate "no-barrier" scenarios, which are intended to provide an upper bound criticality probability to address the uncertainty in barrier performance which currently exists.

With all of the pointwise probabilities of the top event (waste package criticality) determined, the cumulative distribution can be created. Figure 7.19 displays the cdf for the occurrence of a waste package criticality event for both the barrier and no-barrier scenarios (TBV-059-WPD). The number of waste package criticalities expected to occur by a given time can be approximated from the distribution simply by multiplying the pointwise probability at that time by the number of packages. In particular, for a repository containing 10,000 UCF-WPs, the expected number of UCF-WP criticalities (with barrier credit) that would have occurred by 200,000 years is 0.99 (TBV-059-WPD) with the WP barriers credited, and slightly over 1.0 without crediting the WP barriers.

Originator: J.R. Massari	Checker: J.K. McCoy
---------------------------------	----------------------------

Table 7.6. Summary of Pointwise Top Event Probabilities and Constituent Cutsets (w/ Barrier Credit)

Time (Years)	Top Event Probability	Cutset Probabilities and Event Sequences				
20,000	5.72E-09	5.722E-09	CRACKSWP	GEOMETRY	HOLES	WPB&LDH20K
40,000	1.35E-06	1.341E-06	CRACKSWP	GEOMETRY	HOLES	WPB&LDH40K
		5.303E-09	CRACKSWP	GEOMETRY	HOLES	WPB&LDL40K
80,000	3.69E-05	2.062E-05	CRACKSWP	GEOMETRY	HOLES	WPB&LDL80K
		1.233E-05	CRACKSWP	GEOMETRY	HOLES	WPB&LDH80K
		1.970E-06	TECTONC80K	GEOMETRY		
		1.970E-06	CLIMATE80K	GEOMETRY		
120,000	7.26E-05	3.649E-05	CRACKSWP	GEOMETRY	HOLES	WPB&LDL120
		2.660E-05	CRACKSWP	GEOMETRY	HOLES	WPB&LDH120
		4.750E-06	TECTONC120	GEOMETRY		
		4.750E-06	CLIMATE120	GEOMETRY		
160,000	8.84E-05	3.725E-05	CRACKSWP	GEOMETRY	HOLES	WPB&LDL160
		3.501E-05	CRACKSWP	GEOMETRY	HOLES	WPB&LDH160
		8.090E-06	TECTONC160	GEOMETRY		
		8.090E-06	CLIMATE160	GEOMETRY		
200,000	9.90E-04	3.726E-05	CRACKSWP	GEOMETRY	HOLES	WPB&LDL200
		3.592E-05	CRACKSWP	GEOMETRY	HOLES	WPB&LDH200
		1.290E-05	TECTONC200	GEOMETRY		
		1.290E-05	CLIMATE200	GEOMETRY		

Table 7.7. Summary of Pointwise Top Event Probabilities and Constituent Cutsets (w/o Barrier Credit)

Time (Years)	Top Event Probability	Cutset Probabilities and Event Sequences				
20,000	2.60E-06	2.451E-06	CRACKSWP	GEOMETRY	HOLES	WPB&LDL20K
		1.494E-07	CRACKSWP	GEOMETRY	HOLES	WPB&LDH20K
40,000	2.17E-05	1.825E-05	CRACKSWP	GEOMETRY	HOLES	WPB&LDL40K
		2.784E-06	CRACKSWP	GEOMETRY	HOLES	WPB&LDH40K
		3.360E-07	TECTONC40K	GEOMETRY		
		3.360E-07	CLIMATE40K	GEOMETRY		
80,000	6.17E-05	4.005E-05	CRACKSWP	GEOMETRY	HOLES	WPB&LDL80K
		1.597E-05	CRACKSWP	GEOMETRY	HOLES	WPB&LDH80K
		2.840E-06	TECTONC80K	GEOMETRY		
		2.840E-06	CLIMATE80K	GEOMETRY		
120,000	8.27E-05	4.150E-05	CRACKSWP	GEOMETRY	HOLES	WPB&LDL120
		3.019E-05	CRACKSWP	GEOMETRY	HOLES	WPB&LDH120
		5.500E-06	TECTONC120	GEOMETRY		
		5.500E-06	CLIMATE120	GEOMETRY		
160,000	9.87E-05	4.150E-05	CRACKSWP	GEOMETRY	HOLES	WPB&LDL160
		3.624E-05	CRACKSWP	GEOMETRY	HOLES	WPB&LDH160
		1.050E-05	TECTONC160	GEOMETRY		
		1.050E-05	CLIMATE160	GEOMETRY		
200,000	1.12E-04	4.150E-05	CRACKSWP	GEOMETRY	HOLES	WPB&LDH200
		3.670E-05	CRACKSWP	GEOMETRY	HOLES	WPB&LDL200
		1.710E-05	TECTONC200	GEOMETRY		
		1.710E-05	CLIMATE200	GEOMETRY		

Originator: J.R. Massari	Checker: J.K. McCoy
---------------------------------	----------------------------

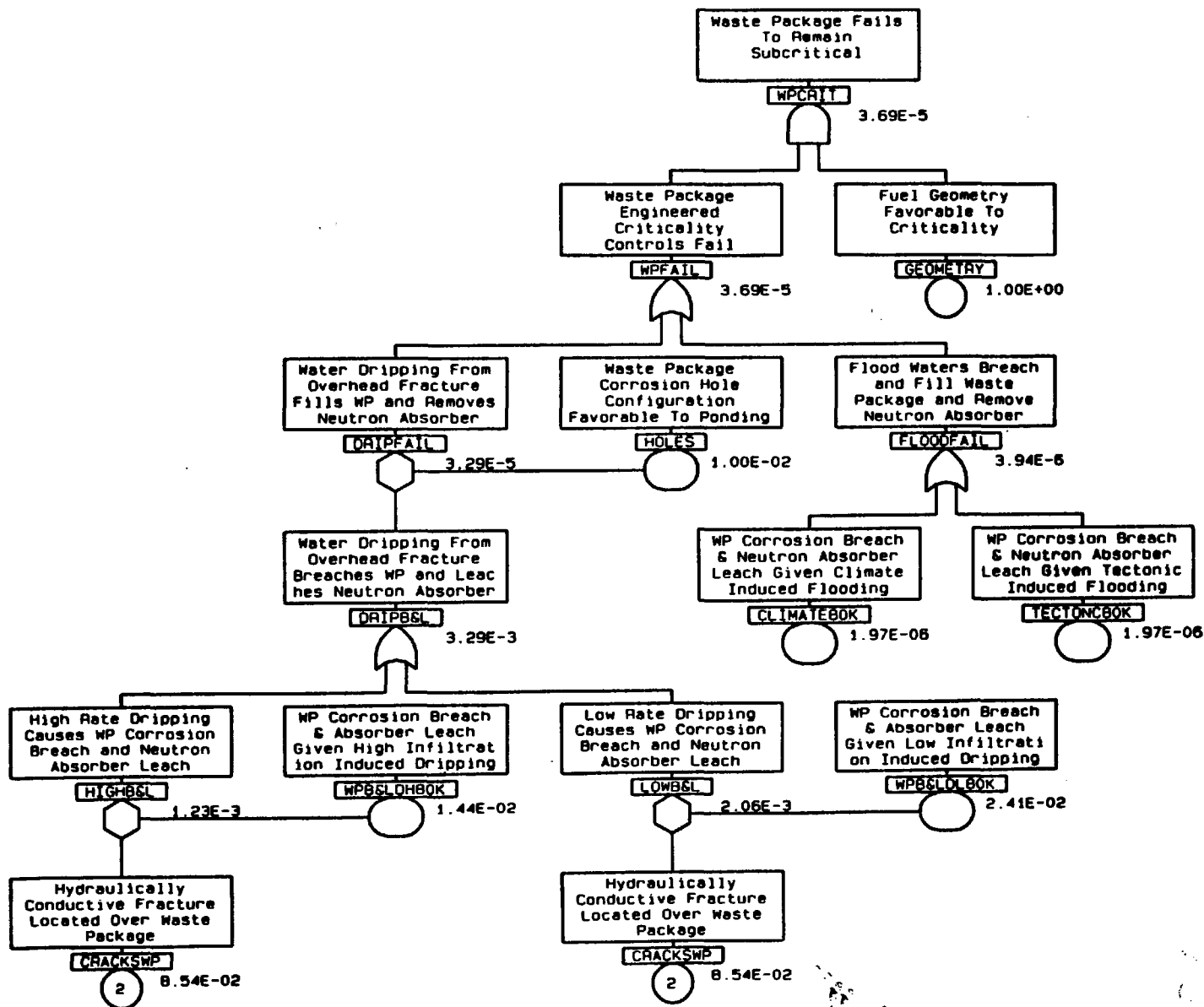


Figure 7.18. Waste package criticality fault tree quantified at 80,000 years after emplacement

Originator: J.R. Massari

Checker: J.K. McCoy

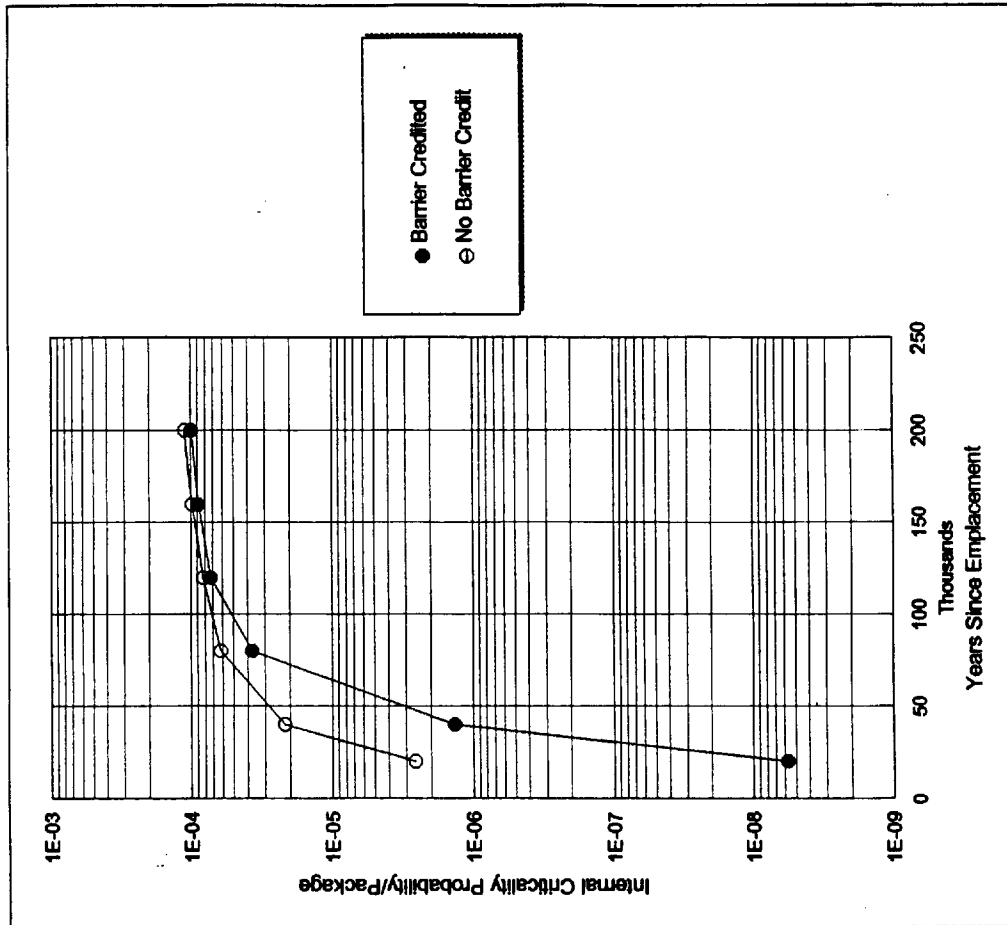


Figure 7.19. Results of fault tree top event quantified at various times since emplacement with and without credit for the waste package barriers (TBV-059-WPD)

Originator: J.R. Massari

Checker: J.K. McCoy

8. Conclusions

This design analysis has established a process for determining the probability of waste package criticality as a function of time, which is described in Section 7. In particular, Section 7.4 describes a methodology for determining the probabilities and pdf's of the events which are essential to the production of a criticality. We have used the established process to estimate the probability of criticality as a function of time since emplacement for the uncanistered fuel waste package (UCF-WP); the results are summarized in the cdf's shown in Figure 7.19. The cutsets presented in Tables 7.6 and 7.7 identify the dominant sequences leading to waste package criticality.

It is obvious from a review of the cutsets presented in Tables 7.6 and 7.7 that the dominant sequences contributing to the rise in the probability of criticality during the first 80,000 years are those involving water dripping on a waste package from an overhead fracture. As mentioned previously in the discussion on fracture frequency in section 7.4, information from the STRIPA validation drift suggests that flowing fractures primarily occurred in regions of high fracture density. Actions taken to identify and avoid placement of waste packages in such areas would significantly reduce the probability that a waste package would be located under such a fracture, and thus reduce the rate and degree to which the overall waste package criticality probability rises in the first 100,000 years. These conclusions however, are subject to validation and/or refinement of the assumptions made in the analysis regarding flowing fracture frequency.

It is also evident from the cdf's shown in Figure 7.19 that the rate at which the barrier is assumed to be breached has a significant effect on the rate at which the criticality probability rises over the first 100,000 years, but little effect thereafter. The effect in the early years is primarily due to the uncertainty in the time-to-breach of the waste packages located below flowing fractures. However, in the later years, further increases in the probability of waste package criticality are primarily governed by the occurrence of events which produce repository flooding. As the time frame for occurrence of these events is on the order of several million years, and the range uncertainty in barrier performance spans at most only a few thousand years, there is little effect on the overall probability of criticality due to sequences initiated by flooding. It should be noted that the probability of criticality continues to slowly rise beyond 200,000 years, reflecting the increasing probability of repository flooding and the assumption that the fuel assembly geometry always remains intact. Future analyses which include external and altered fuel configuration criticality sequences may affect the results for later years.

Finally, the current analysis treated both UCF-WP basket designs identically, by assuming that there was a single 10 mm thickness of borated stainless steel absorber material between assemblies. In section 7.4.3.2, it was assumed that the boron would be leached out of the stainless steel matrix as it corroded from both sides by the process of general corrosion. This assumption is valid for the ILB UCF-WP design, but may be slightly unconservative for the tube basket UCF-WP design. Due to the fact that this design

Originator: J.R. Massari**Checker: J.K. McCoy**

employs 5 mm thick tubes, it would present four surfaces where corrosion of the stainless steel (and thus boron removal) could occur. This would have the effect of reducing the MTTF for the absorber leach distributions by a factor of two, thus slightly raising the probability of criticality at a given time. However, as the outside surface of one tube will be very close to the outside surface of the adjacent tube, there may be no credible mechanism for removal of the boron from the tight space, in which case, the above assumption would still remain valid. Also, the corrosion products may eventually plug the gap, preventing water entry and further corrosion between adjacent tubes. Regardless of which of the above scenario's is true, the tube design still remains bounded by the "no-barrier" case presented in section 7.

While this document does not deal with the consequences of the criticality, it should be noted that, all numerical calculations of such processes published to date indicate that the energy release would be limited to boiling of water at atmospheric pressure, similar to the natural reactor which occurred at Oklo several billion years ago. Such a low grade criticality could continue for thousands of years, but simple calculations show that at an expected number of criticalities less than 1, the inventory of radionuclides accumulated by the criticality at any time during such a criticality would be an insignificant fraction of the nuclides already present in the spent fuel inventory of the entire repository.

9. Attachments

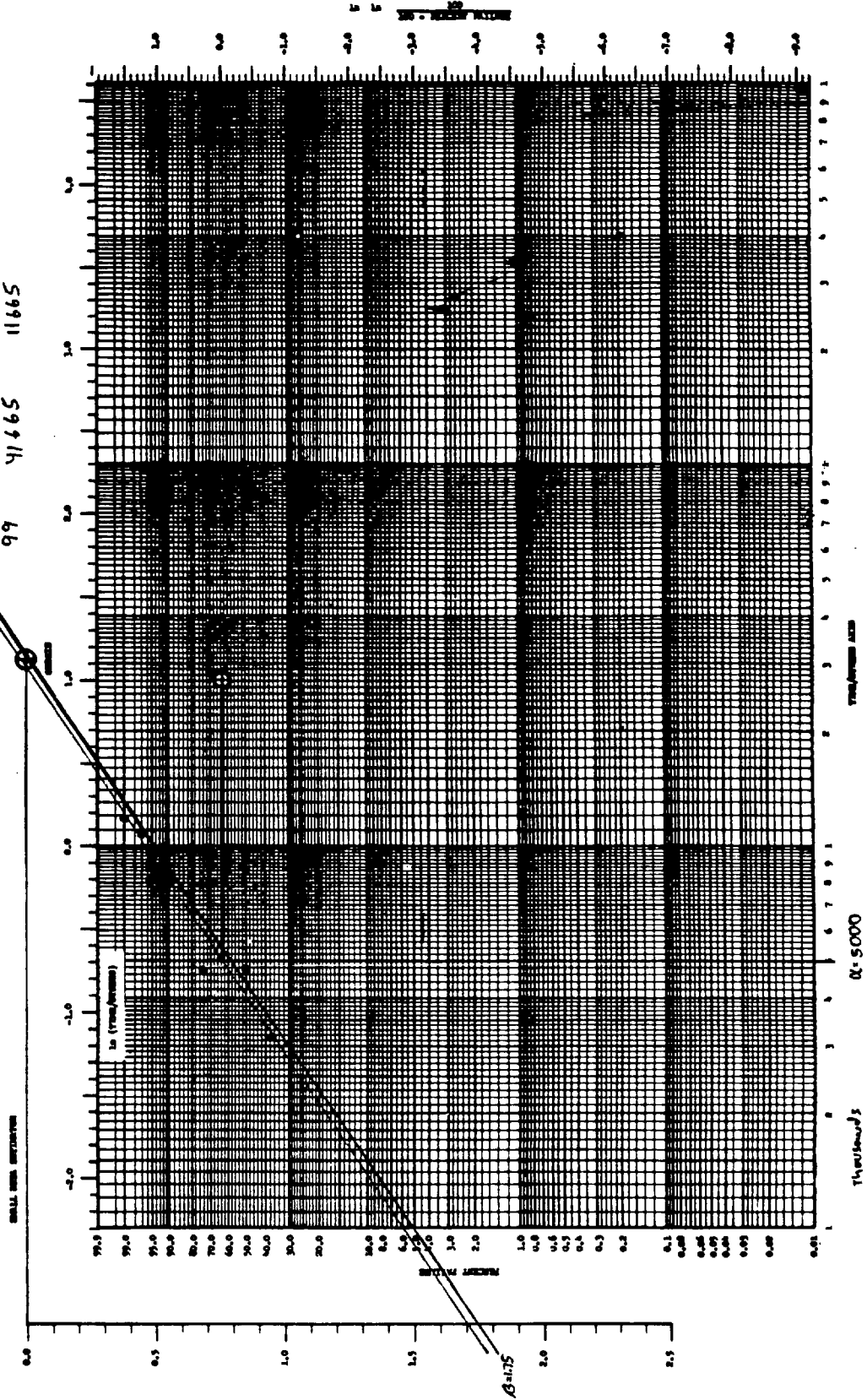
- Attachment I - Weibull Paper Plots of Waste Package Breach Model Data
- Attachment II - CAFTA Version 2.3 Quantification Results Verification
- Attachment III - Independent Verification of Monte-Carlo Convolution

Originator: J.R. Massari	Checker: J.K. McCoy
---------------------------------	----------------------------

Low Drip Conditions $\theta = 30,000$

$\frac{\sigma}{\mu}$	t	$t - \theta$
37.5	33364	3364
50	34807	4807
75	34850	4850
90	38286	8286
97	40843	10843
99	41665	11665

FIG. 11A-2 METALLIC FUEL ELEMENTS (COP-100) - 3-YEAR UNCANISTERED



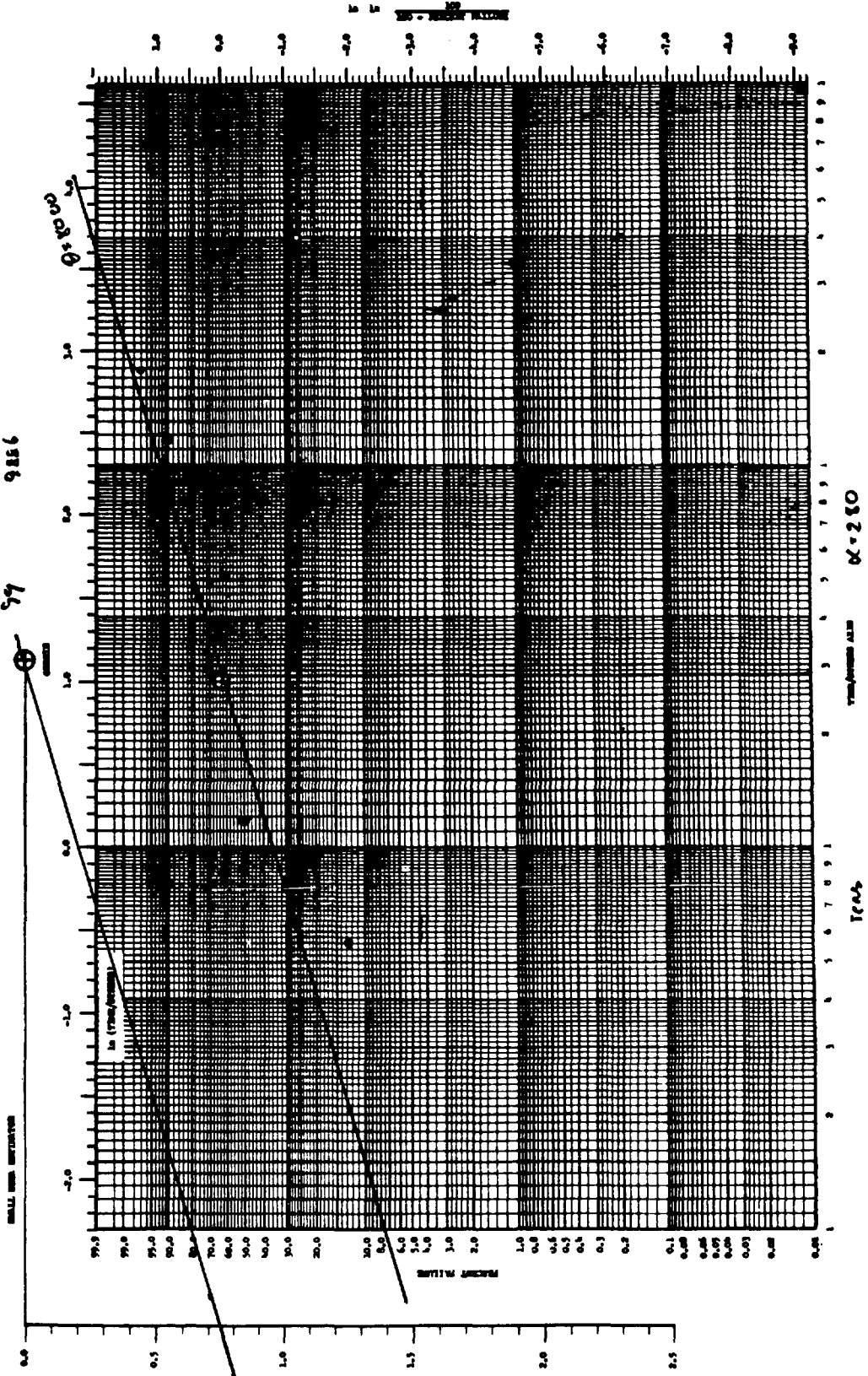
Assume $\theta = 8000 \text{ yrs}$

Flooded Conditions

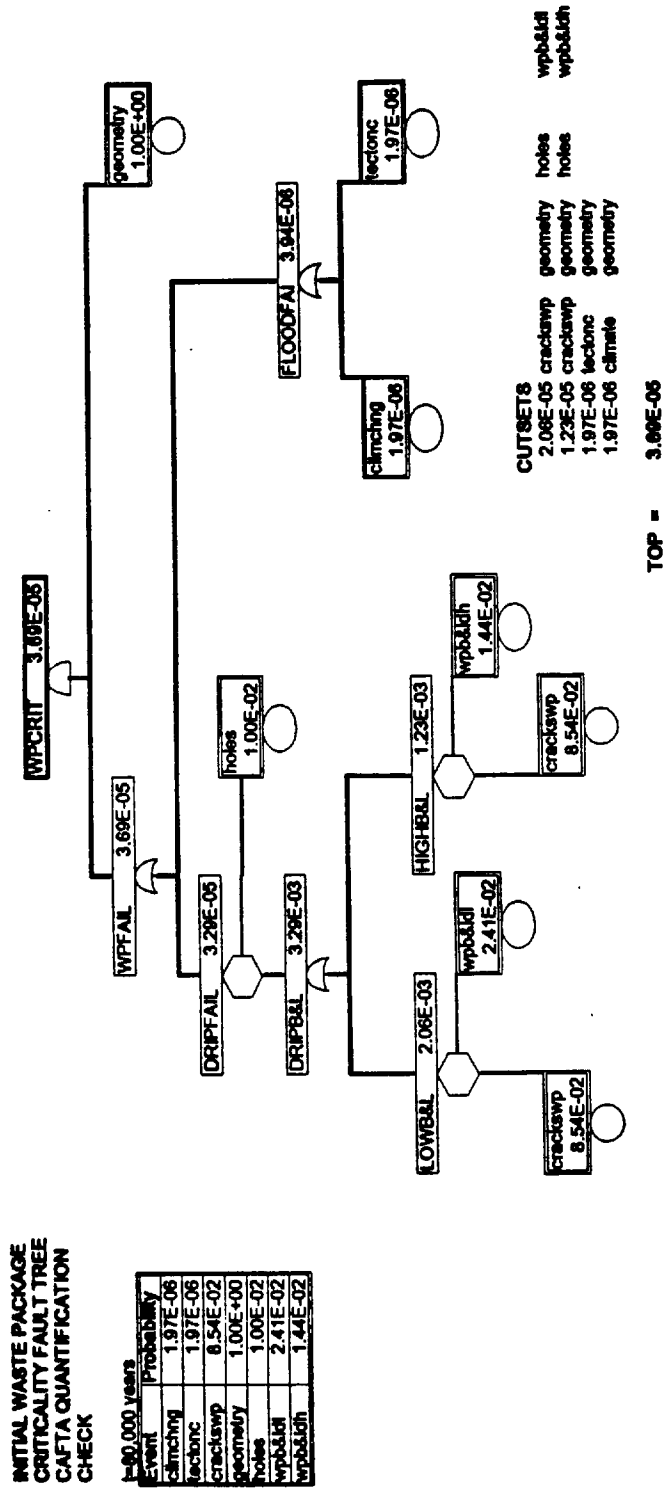
- 12.5
- 50
- 75
- 90
- 97
- 99

- 7052
- 8117
- 8452
- 9181
- 9761
- 9856

Fig. 11B-2 INITIAL PROBABILITY
OF A FAILURE
= 1-CRITICAL PROBABILITY



Originator: J.R. Massari	Checker: J.K. McCoy
--------------------------	---------------------




```

/*This program was used to verify the Monte-Carlo calculation of the two-fold
convolution for the flooding with barriers case. This program does not
apply the fissile fraction correction factor, which can be applied by hand
as is indicated in the listing of the output file.
*/
#include <stdio.h>
#include <math.h>
#include <stdlib.h>
#define DIM 4000
#define LIM 200

float f[DIM]={0},g[DIM]={0},h[DIM]={0},conv[DIM]={0},conv2[DIM]={0},test[DIM];
long int n=DIM;
float dt=50;
float err,merr=0,msqerr=0;
FILE *fout;

main(argc,argv)
int argc;
char* argv;
{long int i,j,k,m;
float csum=0,csum1=0;
fout=fopen("conv.out","w");
if(argc>1)n=atoi(argv[1]);
build();
for(i=1;i<n;i++)
  {for(j=1;j<i;j++)
    {conv[j]=0;
    if(LIM>(i-j))m=i-j;
    else m=LIM;
    if((i-j)>=159)
      for(k=159;k<m;k++)
        {/*printf("%d %d %d\n",i,j,k);*/
        conv[i-j]+=g[i-j-k]*h[k];}
    conv[i-j]+=g[i-j]*h[0]/2;
    conv[i-j]*=dt;
    conv2[i]+=f[j]*conv[i-j];}
  conv2[i]+=f[0]*conv[i]/2+f[i]*conv[0]/2;
  conv2[i]*=dt;
  if(i%100==0)printf("%ld\n",i);}
printf("\n");
fprintf(fout,"CDF's\n");
for(i=1;i<n;i++)
  {csum+=conv2[i];
  csum1+=conv[i];
  if(i%100==0)fprintf(fout,"%10.0f %e %e\n",i*dt,csum*dt,csum1*dt);}
printf("Convolution computed in %d steps\n",n);}

build()
{long int j;
float al=19675,be=2.1,t,th=2400,fsum=0,gsum=0,
al2=280,be2=.75,th2=8000,hsum=0;
fprintf(fout,"input functions\n");
for(j=0;j<n;j++)
  {t=dt*j;
  f[j]=(2e-14)*t;
  if(t>th)g[j]=be/al*pow((t-th)/al,be-1)*exp(-pow((t-th)/al,be));
  if(t>th2)h[j]=be2/al2*pow((t-th2)/al2,be2-1)*exp(-pow((t-th2)/al2,be2));
  fsum+=f[j];
  gsum+=g[j];
  }
}

```

Originator: J.R. Massari

Checker: J.K. McCoy

```
    hsum+=h[j];  
/*  if(j%10==0) fprintf(fout,"%d %e %e %e\n",j,f[j],g[j],h[j]); */  
fsum=(f[0]+f[n-1])/2;  
gsum=(g[0]+g[n-1])/2;  
hsum=(h[0]+h[n-1])/2;  
fsum*=dt;  
gsum*=dt;  
hsum*=dt;  
printf("Integrals of constituent pdf's %f %f %f\n",fsum,gsum,hsum);  
fprintf(fout,"end of input functions\n");}
```

Originator: J.R. Massari

Checker: J.K. McCoy

input functions
end of input functions
CDF's

5000	0.000000e+00	0.000000e+00
10000	0.000000e+00	0.000000e+00
15000	9.923642e-10	3.311449e-02
20000	2.238700e-08	1.546264e-01
25000	1.234353e-07	3.314471e-01
30000	3.903130e-07	5.115181e-01
35000	9.113578e-07	6.548141e-01
40000	1.757652e-06	7.474393e-01
45000	2.975853e-06	7.969245e-01
50000	4.591377e-06	8.189696e-01
55000	6.615825e-06	8.271976e-01
60000	9.053643e-06	8.297774e-01
65000	1.190628e-05	8.304576e-01
70000	1.517412e-05	8.306087e-01
75000	1.885726e-05	8.306367e-01
80000	2.295572e-05	8.306405e-01
85000	2.746951e-05	8.306405e-01
90000	3.239860e-05	8.306405e-01
95000	3.774303e-05	8.306405e-01
100000	4.350277e-05	8.306405e-01
105000	4.967783e-05	8.306405e-01
110000	5.626822e-05	8.306405e-01
115000	6.327392e-05	8.306405e-01
120000	7.069495e-05	8.306405e-01
125000	7.853130e-05	8.306405e-01
130000	8.678297e-05	8.306405e-01
135000	9.544996e-05	8.306405e-01
140000	1.045323e-04	8.306405e-01
145000	1.140299e-04	8.306405e-01
150000	1.239429e-04	8.306405e-01
155000	1.342711e-04	8.306405e-01
160000	1.450147e-04	8.306405e-01
165000	1.561737e-04	8.306405e-01
170000	1.677479e-04	8.306405e-01
175000	1.797374e-04	8.306405e-01
180000	1.921423e-04	8.306405e-01
185000	2.049625e-04	8.306405e-01
190000	2.181981e-04	8.306405e-01
195000	2.318489e-04	8.306405e-01

↑
 Multiply this column by 0.04 (avg. critical fuel fraction)
 to get the approximate value of the probability in
 Figure 7.13